**University of Southern Queensland**

**Faculty of Health, Engineering and Sciences**

# DUMPER DERAILMENT INVESTIGATION AND DEVELOPMENT OF CUSTOM CHECK RAIL

A dissertation submitted by

Lindsay Dobson

in fulfilment of the requirements of

ENG4111 and 4112 Research Project

towards the degree of

Bachelor of Engineering (Honors) (Mechanical)

Submitted October, 2016

# Abstract

Rio Tinto Iron Ore owns and operates the largest privately owned rail system in Australia, with approximately 1700km of mainline, servicing 15 different mine sites. To haul the iron ore from the mines the railway utilises 191 locomotives and approximately 11500 wagons. The ore is loaded into the wagons whereby it is transported via rail to one of 3 ports for export.

The unloading of the wagons at the port is done via a rotary car dumper, whereby the wagon enters the process inside of the dumper and the wagon is turned 100° axially to dump the ore into a chute. Once dumped the wagon is returned to original orientation and evacuated via an indexing arm and the process repeated.

Rio Tinto Iron Ore have experienced regular derailments on the outgoing side of the car dumpers at their Parker Point operations, known as CD3P/CD4P, in the Pilbara since their installation in 2007. The outgoing track section has seen an increased number of derailments in the final quarter of 2015 and again in the first quarter of 2016, adding pressures to find a route cause and solution. As a mitigation measure in 2012 a non-active checkrail was installed in an attempt to return the low leg wheel set to alignment once flange climb had occurred. This has proved to be ineffective with the checkrail at CD3P and CD4P currently installed such that it does not fulfil its intended function. In the current alignment and orientation, the checkrail does not contact the wheel until the opposing wheel has derailed and moved over centre of the high leg rail.

This work investigates existing site conditions at the location and assesses them in line with the generally accepted standards and identifies a root cause.

**University of Southern Queensland**

**Faculty of Health, Engineering and Sciences**

**ENG4111/ENG4112 Research Project**

## Limitations of Use

**University of Southern Queensland**

## Faculty of Health, Engineering and Sciences

## ENG4111/ENG4112 Research Project

## Certification of Dissertation

I certify that the ideas, designs and experimental work, results, analyses and conclusions set out in this dissertation are entirely my own effort, except where otherwise indicated and acknowledged.

I further certify that the work is original and has not been previously submitted for assessment in any other course or institution, except where specifically stated.

Lindsay James Dobson
Student # 0061024815

# Acknowledgements

This project was conducted under the principal supervision of Dr Steven Goh, Senior Lecturer - School of Mechanical and Electrical Engineering, University of Southern Queensland.

I would also like to acknowledge and thank the Rail Engineering and Rail Network Maintenance staff from Rio Tinto whom assisted me in the collection of information and results in challenging circumstances.

Most of all I would like to thank my wife, Shannon and children, Claudia, Lucas and Eva for their continued support and encouraging words during the project.

# Table of Contents

# Table of Figures

# GLOSSARY

| | |
|---|---|
| AAR | Association of American Railroads |
| ONRSR | Office of the National Rail Safety Regulator |
| IOC | Instrumented Ore Car |
| $\mu$ | coefficient of friction |
| $\alpha$ | Yaw angle |
| $V_t$ | Lateral velocity of a wheelset |
| $\omega$ | Angular velocity |
| r | rolling radius |
| $\theta$ | Wheelset angle of attack |
| $\beta$ | Wheel flange angle |
| L | lateral force at wheel flange |
| V | Vertical load on the wheel |
| N | Force normal to flange angle |
| PoD | Point of Derailment |
| CD3/CD4 | Car Dumper #3/Car Dumper #4 |
| PP3/4ECL | Parker Point CD3/CD4 empty car line |
| PPCD3LCL | Parker Point Car Dumper 3 Loaded Car Line |
| PPCD4LCL | Parker Point Car Dumper 4 Loaded Car Line |

# Chapter 1 INTRODUCTION

Rio Tinto has installed checkrails at the location CD3P and CD4P as a measure to stop derailments due to flange climb on the tight radius curve on the outgoing side of the car dumpers. The checkrails were installed in 2012 following 4 derailment events within the first 6 months of the year. Following the installation, it appeared that the mitigation measure had been effective with only 1 derailment occurring in the following 12 months. Since this time the number of derailments at this location has continued to rise and has in 2016 surpassed the numbers that had been experienced in 2012, with 6 events occurring in the first 6 months of the year.

## 1.1 Project Objectives

The aim of this report is to identify the contributing factors and root causes of repeated derailments that have occurred at Rio Tinto's Car Dumper 3P and Car Dumper 4P at Parker Point, Dampier Western Australia. The report considers the existing site conditions and identifies the potential rectification measures.

The report focuses on the design and function of the existing checkrail, due to generally held belief that the checkrail installed is ineffective and is failing to perform its intended function. The intent is to determine if modification of the existing checkrail is warranted and if so, identify the parameters requiring change and develop a fit for purpose checkrail to mitigate the derailment risk. This report also identifies probable contributing factors to the derailments and outlines the containment options available to rectify these.
The scope of the project is:

- To investigate the underlying causes and site specific conditions contributing to the regular derailments at CD3 and CD4.
- Develop a rectification methodology, including the development of a replacement fit for purpose checkrail if deemed the appropriate control.
- Identify and deliver maintenance recommendations for the new checkrail and track section.

## 1.2 Background

Rio Tinto Iron Ore Pilbara operations maintain 3 ports as part of their export operation. In order to transport the iron ore from inland mine sites to the port, in preparation for export, the ore is loaded onto trains at the mine and transferred to the ship loading facilities via the rail network.

Once at the port the ore is offloaded via a rotary car dumper, whereby the rail wagon is held to the section of isolated track and rotated so that the contents of the wagon are emptied. Once emptied the unloaded wagons, whilst still attached to the remaining consist, are evacuated from the car dumper section via an indexing arm that forces the wagon through the outgoing (empty) side of the process. Once all wagons are unloaded the consist will be returned to the main running line under the power of locomotive by travelling back through the Parker Point CD3/CD4 empty car line.

The outgoing track sections at Parker Point -1.18km PPCD3LCL and -1.18km PPCD4LCL have a history of derailing empty ore wagons since the dumpers were commissioned in 2007.

The below, figure 1 shows the the total count by year of known derailments on the outgo side of CD3P and CD4P, of which most have identical symptoms.

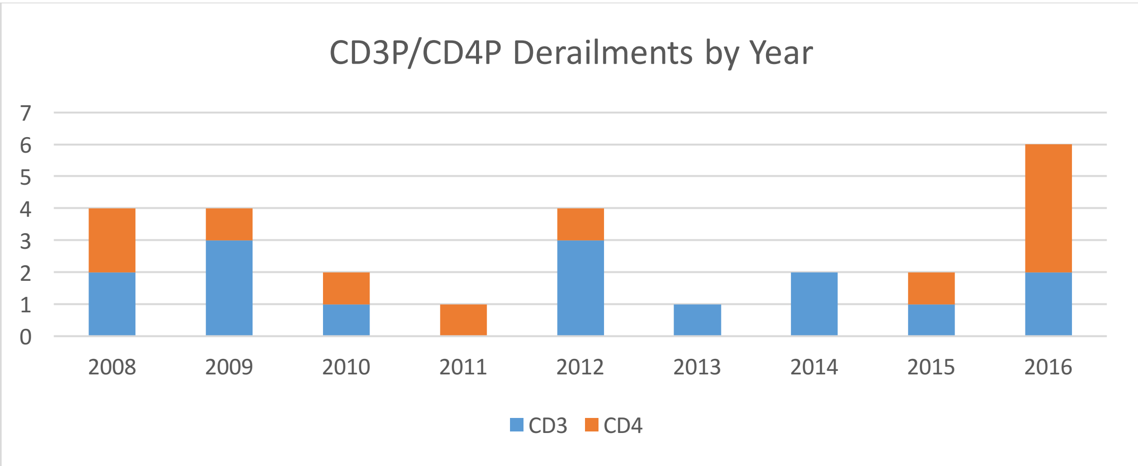


*Figure 1: CD3P/CD4P Derailment History*

## 1.3 Financial Costs of Derailment

The delay accounting records from the Parker Point dumpers reveal that there has been an average of 15 trains or 450,000 tonnes lost per year as a result of derailment delays from 2008-2016. This time delay and cost is not inclusive that associated with derailment clean up or repairing track damage. There have been multiple occurrences at the location whereby the section has been closed for more than 2 days whilst investigation and clean-up is undertaken. Not including these major events, the average delay due to minor derailment is 4.5hours.

Presuming that the iron ore price has been at the current spot price of $55/tonne and the losses only include the 450,000 tonnes, the annual cost to the business is in the order of $24M.

# Chapter 2 LITERATURE REVIEW

## 2.1 Derailment

Derailment on any railway is a significant event. In Western Australia all derailments are reportable to the Office of the National Rail Safety Regulator in line with s.57 of *Rail Safety National Law (WA) Regulations 2015.*

Derailments are classified by the regulator as; "Where one or more rolling stock wheels leave the rail or track during railway operations."

*Figure 2: CD3P Derailment Feb 2016*

According to the RISSB Derailment Investigation and Analysis Guideline there are many causes of derailment. The typically accepted immediate causes are listed below:

- Wheel obstruction,
- Wheel(s) lifted off the rail,
- Rail gauge widening, Wheel(s) drop between rails
- Wheels rotate over rail (vehicle overturning),
- Flange or wheel climb.

The above derailment mechanisms can be summarised as:

- Wheels lifted off the rails – large forces or shocks in the train (sudden applications of power or take up of slack in the train draft gear), braking shocks, collision, wagons squeezed up, axle journal shears off, obstruction to bogie, or collapse of a safety critical part of the vehicle.

- Rail gauge widening – this requires failure of the rail or the rail fastening/support, or the wheel moving on the axle.
- Wheel obstruction – a physical obstruction of the wheels or bogie by relatively small objects e.g. ballast or dislodged rolling stock components. Wheels are deflected from the rails or the flangeway is lifted.
- Wheels rotate over the rail – this is associated with overturning of the vehicle (rollover). The most common cause being excessive speed on a tight curve.
- Flange climb – a change in the train forces and conditions at the wheel flange/rail contact point that leads to the flange climbing and crossing the rail. Typically, from a large reduction in wheel load (V), high lateral force (L) from single factor or combination of factors involving vehicle, track geometry, train handling.

Additional mechanisms for derailment can occur at the locations of points and switches on a network, however this is not relevant to this location and is not further considered.

## 2.2 Wheel – Rail-Wheel Interface theory

The interface between rail and wheel on the railway is an extremely complex system. During normal operation the interface between the wheel and the rail is a small horizontal contact patch of approximately 1cm$^2$ and is subjected to very high stresses. This location continuously varies with the movement of the train as it progresses down the track. The possible regions for Wheel rail contact and the typical corresponding conditions are taken from Tournay, 2001 and shown in figure 4, with figure 3 showing the typical contact stresses for the wheelset when entering a Right hand curve.

The understanding of wheel-rail interface has typically been demarcated between civil engineers, dealing with the rail and foundations, and mechanical engineers dealing with the wheel and vehicle. Whilst the basic principal of wheel – rail system is that of a flanged wheelset rolling along a rigid steel track the irreversibility of the process dictates that a systems based approach is best served to solving the problems involving rail wheel interface. Full understanding of wheel–rail contact is extremely complex and is beyond the scope and requirements of this project.

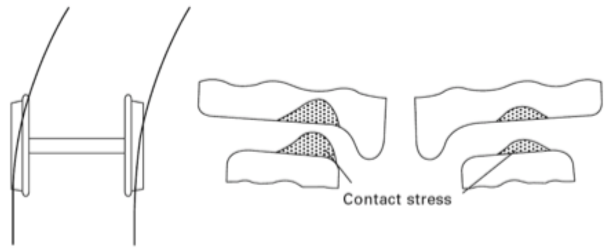


*Figure 3 Contact stress for wheelset entering RH curve*

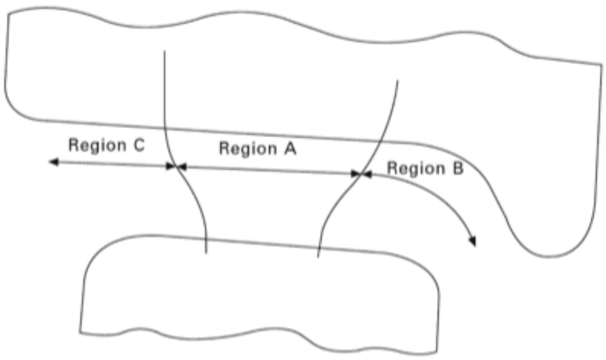


*Figure 4 Wheel - Rail contact zones (Adapted from Tournay, 2001)*

**Region A – Wheel tread contacts rail head**; The wheel – rail contact is made most often in this region and usually occurs when the vehicle is running on straight track or very high radius curves. This region yields the lowest contact stresses and lateral forces.

**Region B – Wheel flange contacts rail gauge corner**; The contact in this region is much smaller than in region A and is often more sever. Typically wear rates and contact stresses are much higher.

**Region C – Contact between field sides of wheel and rail**; Contact is least likely to occur here. If contact does occur, high contact stresses are induced and undesirable wear features occur. This leads to incorrect steering of the wheelset.

## 2.3 Wheelset

For simplicity, a wheelset can be described as two conical, nearly cylindrical wheels, linked together with a rigid axle. To prevent derailment by simply running off the track, each wheel has a flange located on the track center line side of the wheel. In straight line running the flanges do not contact the rail head, however will go to rail flange contact with the rail gauge corner in curves.

The rigid link between the two wheels would indicate that the railway wheelset is designed only to go straight ahead but in order to have the wheelset negotiate curves the tread profile of the wheelset is designed with a slight taper from the flange to the outside of the wheel. This means that the largest wheel tread diameter is closest to the flange and in cornering the wheelset will have the flange of one wheel forced into contact with the rail and the other wheel on the axle will then run on the outer section of the tread. The net effect being that the wheelset will be running on wheels of different diameters and therefore assist curve negotiation.

Rio Tinto wheels run a 3.4mm taper with 900mm radius over 43.5mm and a ±0.25mm tolerance. The full profile can be seen in Appendix B.

## 2.4 Wheelset degrees of freedom

Assuming in this instance that the track is rigid, the wheelset has only the degrees of freedom as illustrated in figure 5:
Where;

- Lateral displacement (y) and,
- Angle of attack, (θ) or as shown in figure 5 (α)

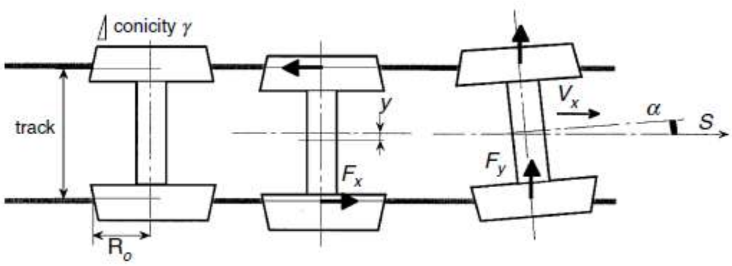


*Figure 5: Wheelset degrees of freedom (Ayasse & Chollet 2006)*

The Wheelset Angle-of-Attack (AOA) is defined as the angle (θ) between the axis of rotation of the wheelset and a radial line in a curve or a line perpendicular to the track centreline on tangent track.

The lateral displacement and the angle of attack are considered as two small displacements relative to the track and taken at the centerline. The amount of displacement, known as ‘play’ will be the limit, of the lateral displacement between the two flange contacts. For Rio Tinto wheelsets, this is generally in the order of 8 mm, dependent on the flange wear.

## 2.5 Theory of Flange Climb and L/V

The most commonly accepted theory for L/V ratio is Nadal’s as described in section 2.9. In addition to the equation by Nadal there have been a number of studies that support the notion, including work by Wu and Wilson 2006, that flange climb derailments generally occur on curves. This is due to the wheels on the outer rail, known as the high rail, experiencing a base level of lateral force to vertical force ratio (L/V) related to:

- Curve radius,
- Wheel profile,
- Bogie suspension characteristics,
- Vehicle speed.

These factors combine to generate a base wheelset angle of attack (AoA), which in turn generates the base level of lateral curving force. When the L/V ratio exceeds the capabilities of the wheel, flange climb occurs.

Factors contributing to high L/V ratios are listed below:

- Track misalignments including twist over the bogie and variations in super elevation
- Torsionally stiff vehicles operating on track with excessive twist
- Excessive super elevation
- Lateral or longitudinal vehicle loading imbalances
- Sever flat spot on wheel

## 2.6 L/V Ratio

The lateral to vertical force ratio (L/V) is the lateral force pushing outward against the rail divided by the vertical force pushing downward on the top of the rail. The L/V ratio gives an indication of the likelihood of derailment due to flange climb and also rail lateral displacement and rollover. The tendency for derailment increases as the L/V ratio increases. This concept is important for understanding these derailment mechanisms.

The L/V ratio will increase if the lateral force increases and the vertical force remains constant, or if the vertical force decreases and the lateral force remains constant. High lateral forces are usually accompanied by high vertical loads, which keep L/V ratios below critical level. The highest L/V ratios most often occur because of a sudden reduction in vertical load.

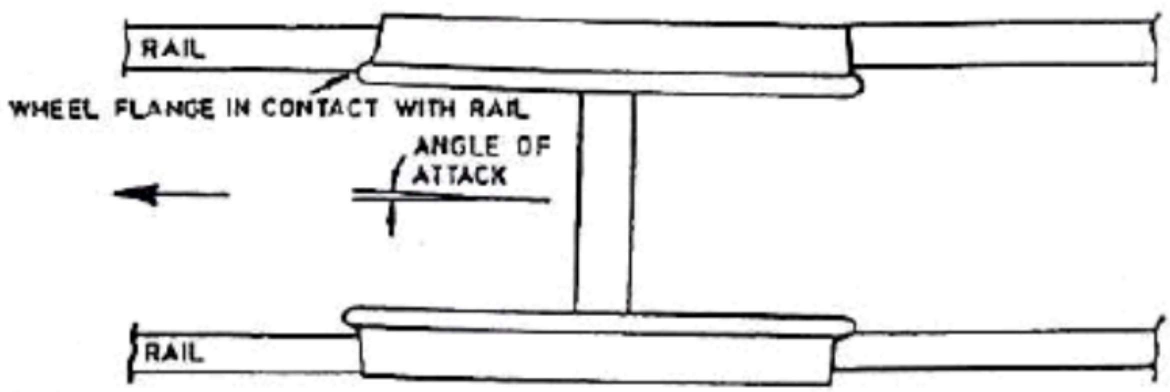


*Figure 6:Wheelset angle of attack (AoA)*

## 2.7 Wheel creep

When a wheel is rotating there are a number of forces generated that influence the wheel motion. A centrifugal force acts on a rail vehicle as it negotiates a curve. The superelevation of the high rail causes gravity to provide part of the force to react to the centrifugal force. The uncompensated centrifugal force on a vehicle as it negotiates a curve has to be balanced by the wheel-rail forces. The high rail bears larger lateral forces than the low rail because of the action of the unbalanced centrifugal force and lateral creep forces caused by axle angle of attack. The creep force alone, due to angle of attack is rarely sufficient to cause the wheel to derail, however need to be understood as it can be sufficient to stop the wheel from falling back and stopping derailment.

Lateral creep is influenced by the angle of attack through a component of the wheelset's rotational velocity. If there is lateral velocity in addition to the velocity set up by the wheels' rotational velocity the net lateral velocity is given by:

$$V_y = y - \omega r \theta \quad (1)$$

The rotational velocity is given by:

$$V_t = -\omega r \sin(\theta) \quad (2)$$

Lateral creep can be defined as the wheel–rail relative lateral velocity divided by the forward velocity.

$$\gamma_y = \left(\theta - \left(\frac{\dot{y}}{V}\right) sec\delta\right) \quad (3)$$

where $\theta - \left(\frac{\dot{y}}{V}\right)$ is the effective angle of attack as a function of the wheelsets lateral velocity, $V_y$. The term sec(δ) always has a positive value during flange climb and the direction of the lateral creep is dependent on the sign of the term $\theta - \left(\frac{\dot{y}}{V}\right)$. From equation (3) it can be seen that the lateral creep equals zero when θ equals $\frac{\dot{y}}{V}$.

The lateral creep changes direction when $\theta < \frac{\dot{y}}{V}$.

Figure 7. by Wu and Wilson shows the three phases or the flange climb process.

Phase 1, left hand illustration, the wheel is under a lateral force and the wheel moves right initiating flange contact with the rail. A lateral creep force is produced and acts on the wheel to oppose flange climb.

Phase 2, the flange contact angle is increased and the wheelset lateral velocity decreases. This results in the lateral creep and creep force reversing direction due to the change of sign of the effective angle of attack in which the lateral force is assisting the wheel to climb.

Phase 3 occurs once the maximum contact angle has passed, the wheelset lateral velocity increases resulting in rapid lateral displacement of the wheelset. This results in the effective angle of attack approaching zero and changes sign. This leads to the lateral creep and creep force changing direction and the lateral creep forces now oppose the wheel climbing motion.

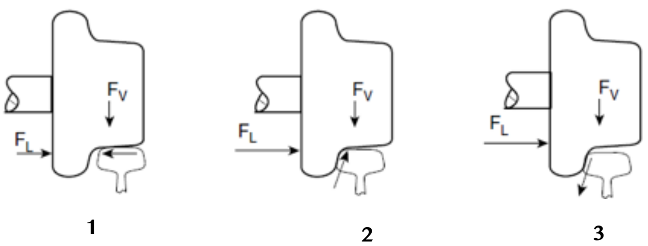


*Figure 7: Flange climb process (Wu & Wilson 2006)*

## 2.8 Flange Climb Distance Criterion

In practice, a flange climbing derailment is not instant. The L/V ratio has to be maintained while the climbing takes place. If the lateral force returns to zero before the flange has reached the top of the rail, the wheel might be expected to drop down again. When the flange contacts the rail for a short duration, as may be the case during hunting (kinematic oscillations) of the wheelset, the L/V ratio might exceed Nadal's limit without flange climbing. For that reason, the flange-climb-distance criteria were developed to evaluate the risk of derailment associated with the wheel L/V ratio limit. Flange climb derailment would occur only if both wheel L/V ratio limit and distance limit are exceeded.

In general, a larger angle of attack reduces the distance required for flange climb derailment as shown in Figure 8: Relationship between climb distance and angle of attack. Hence by bringing the check rail closer, the climb distance increases. This means that high lateral forces have to act on the bogie for a longer period of time to cause a derailment.

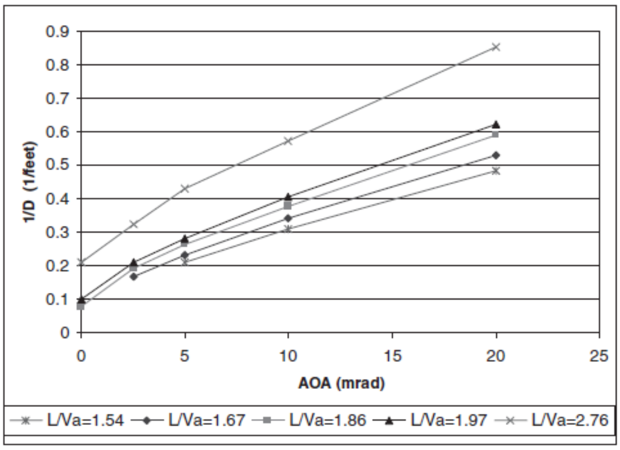


Figure 8: Relationship between climb distance and angle of attack

## 2.9 Nadal Equation

In 1896 M. J. Nadal proposed the railway design equation relating downward force of the wheel upon the rail, to the lateral force of the wheel flange against the face of the rail. This equation is universally used to determine the maximum ratio of lateral force to vertical force before derailment may occur.

The equation is given by:

$$\left(\frac{L}{V}\right) = \frac{\tan(\theta) - \mu}{1 + \mu \times \tan(\theta)}$$

Where L is the lateral force, V is the vertical force, θ is the wheel rail contact angle between the line of action and the horizontal and μ is the dynamic coefficient of friction. When the

Nadal Limit is exceeded for a period of time derailment can occur. Hence the Nadal limit gives the ratio of the maximum lateral force to vertical force that can occur before there is a risk of derailment. It is generally accepted that the lateral force should not exceed 50% of the Vertical force to reduce the likelihood of derailment. It is clear from this criterion that wheels with low flange angles and high coefficients of friction are at a higher risk of derailment.

Nadal's theory is generally accepted as the defining value for instances where the AoA (θ) is greater than 5mrad or the AoA is at an unknown value, as is generally the case for live track. For values less than 5mrad that can be measured can be treated less conservatively

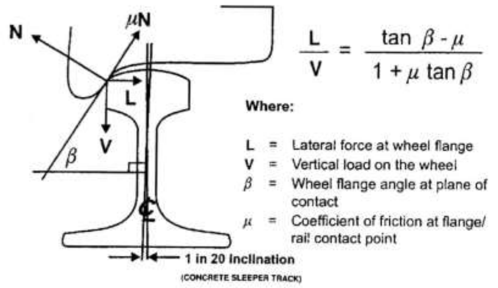


*Figure 9 Flange climb components (RISSB 2013)*

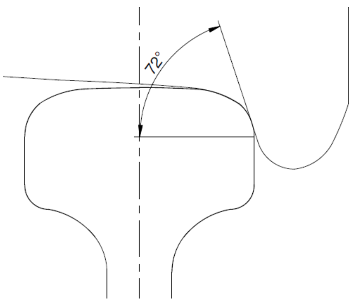


*Figure 10: Contact angle for a new wagon wheel*

## 2.10 Nytran Plot

The multiple angles on railcar wheels make them difficult to position on the track mathematically. Instead graphical techniques such as Nytram diagrams and track diagrams can be used to assess the positioning of the wagon.

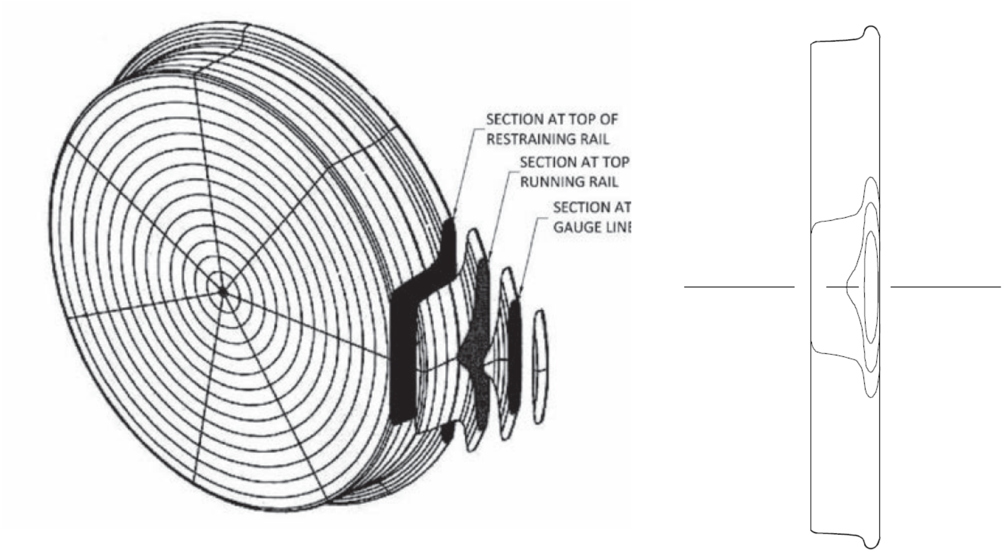


*Figure 11: Illustration of Nytram diagram*

Nytram diagrams are constructed by taking 3 slices through the wheel. One is done at the gauge face of the rail (15.9mm down from the rail head by North American standard), another at the top of the rail and the third at the top of the check rail. These profiles are then mapped on onto a two-dimensional drawing of the wheel. From this drawing, wheels can then be spaced as if they were on a bogie and placed onto track.

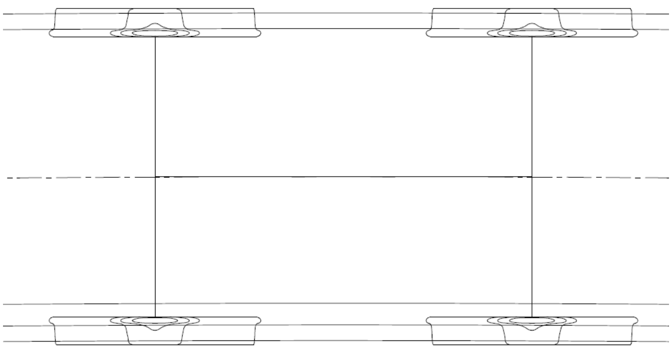

*Figure 12: Example of wheel set placed on track*

The bogie can then be moved around on the track to replicate the situation when it is cornering.

## 2.11 Track Misalignment

A derailment due to track twist in a curve can happen because the misalignment causes the vertical downward forces on the front wheels on one side of the wagon and the opposite side rear wheels to reduce. Track twist is the difference in cross level between two points on the track. The report states a flange climb derailment can occur in a curve if the track is twisted which is consistent with Wu and Wilson 2006.

## 2.12 Torsionally Stiff Vehicles

Tyrell, Weinstock and Greif in a report for the US Department of Transportation state that track twist can lead to derailment for stiffly sprung vehicles. Light vehicles with stiff springs, creating a torsionally stiff vehicle, are generally more susceptible to wheel unloading. Rio Tinto places strict parameters around twist at 2m (short twist) and at 8m (long twist) for mainline track. These can be seen in the Appendix.

## 2.13 Superelevation

Superelevation is where a track is banked into a curve to assist in vehicle corning. An example on super-elevation can be seen in Figure 13.

Excessive superelevation on slow speed curves decreases the force on the wheels running on the high rail due to the change in the centre of gravity (COG) toward the inner rail (low leg). This increase in L/V ratio increases the likelihood of wheel climb.

To steer through a curve there must be lateral forces on the flanges and if the unloading of the vertical forces is greater than what is necessary to overcome the lateral forces the flange will climb the rail.

It is possible to alter track Track super-elevation to reduce derailment likelihood.

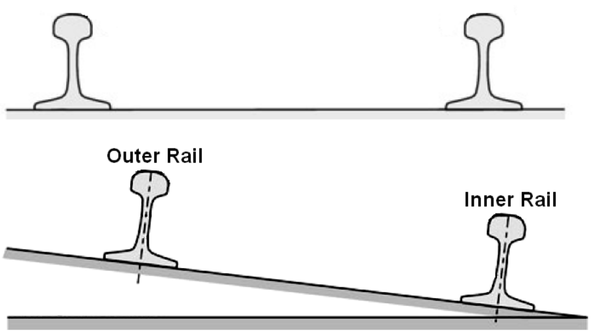


*Figure 13 (Left) Level track, (Right) - Track with Super-elevation*

Increasing the track superelevation of the curved track following the dumpers would reduce the force which the outer wheel flange bears against the outer rail, and therefore would also reduce its tendency to climb the rail. A gradual reduction in the height of the low rail relative to the high rail would provide super elevation which may be beneficial to reduce the risk of derailments at this location. Alteration of track superelevation alone will not stop derailment in this area. The continued existence of a relatively abrupt dip will lead to uplift of the following wagon as the average height of the previous wagon is lower down, and therefore this combination will generate vertical as well as horizontal forces.

The presence of vertical dips continues to elevate the risk of vertical unloading, as the compressive forces now have a vertical component due to the change in angle from one wagon to another at the dip.

Other measures have been suggested as options to reduce the risk of derailment at the dumpers, including placement of a liner on the check rail to close the gap between the back face of the wheel, or a reduction in the incidence of sticky brakes. However, both of these have issues as containment measures. The closure of the gap at the check rail may work in the short term measure, but this is an unproven approach, and may introduce new issues that are not anticipated, not least being that any vertical dips may be allowed to progress to comparable or worse levels rather than being resolved.

## 2.14 Checkrail

To reduce the likelihood of flange climb derailment, check rails, also known as restraining rails, are used in railway systems.

A checkrail or restraining rail is primarily installed to reduce the likelihood of flange climb derailment on the high leg of a curve and secondarily installed for the purpose of providing additional steering action by using the flange of the wheel that is on the inside of the curve. In addition to increasing the track's resistance to flange climb derailment they are also to reduce rail wear in sharp curves, where the high rail wears rapidly. The use of active checkrails is considered beneficial in reducing the frequency of rail replacement and therefore reduces the maintenance frequency and cost of high-rail replacements. The Checkrail assists in guiding any vehicle around the curve by constraining the face of the leading inner wheel against it at the same time as the outer wheel flange bears against the outer rail.

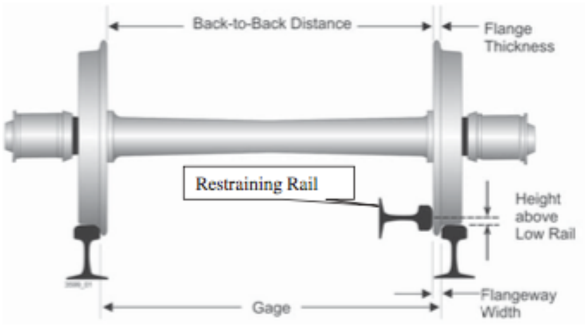


*Figure 14 Wheel and horizontal restraining rail geometry*

The use of a checkrail will reduce the tendency for the outside wheel to derail by climbing the high rail. The use of a checkrail will reduce the lateral force of the opposite outside wheel flange. The extent of this reduction will be dependent on the type of checkrail utilised. The three types of checkrail are summarised below.

1. Active restraining rail: Defined as the restraining rail that reduces the angle of attack (AOA) by more than 50%.
2. Semi-active restraining rail: Defined as the restraining rail that reduces the AOA by 50% or less, preferably between 40% ~ 50%.
3. Passive restraining rail: Defined as the restraining rail that does not reduce the AOA. In other words, it plays a passive role in steering the wheel.

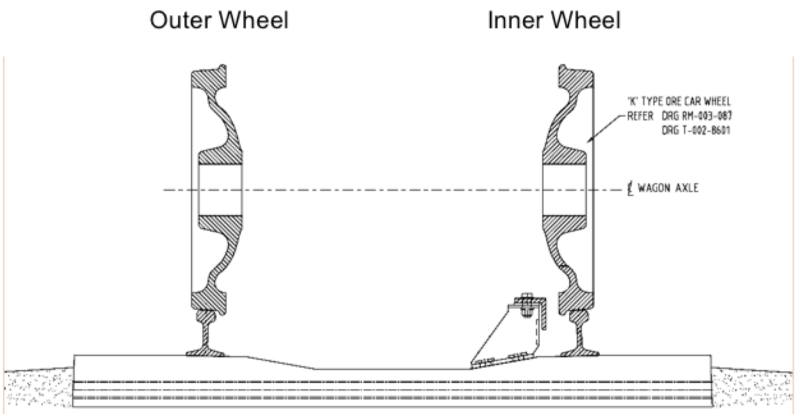

## 2.15 Track lubrication

### 2.15.1 Friction/Adhesion Control

Friction levels at the rail-wheel interface have a significant impact on the performance of wheel and rail components, not only in terms of wear and the development of rolling contact fatigue (RCF) damage, but also through the influence on the dynamic behaviour of the vehicle (i.e. steering), noise and propensity for flange climb.
The major benefits of applying lubrication are;

- Reduced wheel/rail wear
- Reduces noise
- Reduced wheel climb derailment

The reduction in wheel climb derailment impact can be seen directly in the Nadal equation. There are numerous suppliers of friction modification/lubrication equipment, however the three main options include:

a) *Grease Lubrication:* A typical grease lubrication system consists of an applicator bar fitted to the gauge corner of the rail, a pump & reservoir and an activation device (electronic or mechanical). Grease is applied to the gauge corner region of the rail, thus lubricating a targeted area normally exposed to high creepage which subsequently reduces the risk of flange climb. An alternative to wayside installation is through regular manual application of grease onto the gauge corner of the rail. This can either be through hand operation or via specially designed hi-rail equipment, and while possibly the cheapest option, the performance is often limited.

b) *Top of Rail Friction Modifier:* Friction modifiers may also be applied to regulate the friction level to within a 0.3-0.35 adhesion limit. Product is applied to the rail via applicator bars, in a similar manner to the grease but targeting the top of the rail as opposed to the gauge corner only. The product is usually water based, thus limiting the effects in surrounding environment. However, the performance and coverage of friction modifier product may be limited if under occasional traffic only. Hi-rail application options are also available.

c) *Locomotive Flange Lubrication:* is typically recommended for mainline operations, solid state flange (stick) lubrication on locomotive leading wheelsets can, over time, help to lubricate the gauge corner/flange contact region, thus increasing the required L/V ratio necessary for flange climb. This application would be difficult on the outgo side of the car dumper due to the low volume of locomotives traversing this area

If a wayside lubrication system is to be used, it is important that the product is only applied during wagon movements into the curve itself. Disadvantages of any lubrication/friction modifier system include; the ongoing cost and maintenance associated with these devices and carry-over or leakage onto other sections of rail or track work. Regular maintenance is required to keep these systems operational and also clean up any carry-over onto the stock rail.

# Chapter 3 METHODOLOGY

Information gathered in the literature review stage indicates that the most probable cause of wagon derailment at CD3P and CD4P is flange climb. This methodology will review the existing site conditions and available data from the last derailment in a systematic manner consistent with the guidelines provided in AS4292.7 “Railway Safety Management” and compare them to the intended design criteria for this track section. The wheel profile will be measured for the first derailed wagon and the rail profile at the last derailment point. This will be measured and compared to the new rail profile. The methodology will also consider the wayside detection system results, CITEC dumper profiles and IOC data available and consider any inconsistencies.

The optimal checkrail gap will also be calculated using recorded data as part of the methodology.

## 3.1 Existing Conditions

The existing track consists of 68kg/m rail fastened to concrete sleepers with Pandrol e-Clips. A concrete apron has been built outside the dumper by concreting in the existing sleepers. The concrete section transitions rapidly from concrete embedded sleepers to direct laid concrete sleepers on ballast to a depth of approximately 120mm. The ballast in the section of interest is heavily fouled with iron ore fines and is not considered free draining.

The outgoing side of car dumpers CD3P and CD4P are unique in their layout due to the immediate transition into a curve from the dumpers. The track radius trailing from CD3 is recorder as 245m and leads into an opposing radius of 600m before entering the CD3 empty car line according to the design drawing shown in figure 11.

The positioner arm is on the in-go side of CD3P and CD4P. On the outgo side, there is an insulated rail joint directly below the edge of the roof and a concrete pad that comes out 15m from the insulated rail joint. A check rail starts just after the insulated rail joint at the end or the concrete slab and runs for approximately 30m along the curve section of the outgo track until about 600mm south of the -1.3km level crossing. The crossing is made for a single vehicle and has a Dragging Equipment Detectors (DED) either side and a de-railer 24m North of the crossing. The last 3 derailments occurred between the crossing and a single direction de-railer.

Track signaling circuits provide broken rail detection for the main running rails, with additional asset protection provided by monitoring of the rolling stock using DED's at the site. The DEDs on the out go track from CD3P are connected to the dumper control system and stop the dumping process when triggered.

The CD4 and CD3 outgo tracks immediately out of the dumpers is protected through interlocking axle counters with the dumping cycle. Axle counters are used here because this section of track has had issues with current leakage due to the severely fouled ballast. The track gradient exiting the concrete slab was measured -0.017%, where the magnitude of the track gradient increases to -0.041% 500m further along the track.

## 3.2 Last Derailment Site Inspection

The last derailment at CD4P took place at approximately 1155h on 29/06/2016 when the lead wheelset of wagon B25045 (at position 225 of 234 wagons) climbed up the high rail, when it was noticed by rail operations personnel. The dumper operator was notified and halted the dumper indexing operation. By this time leading wheelset of wagon 25045 came off the rails and continued until the wagon came to rest about 6m from the point of derailment, about 20m North of the crossing. It was observed the lateral offset of the wheel from the correct position on track was on the order of 30cm. The overall view of the exit area from CD4P at the time of the derailment is shown in Figure 15.

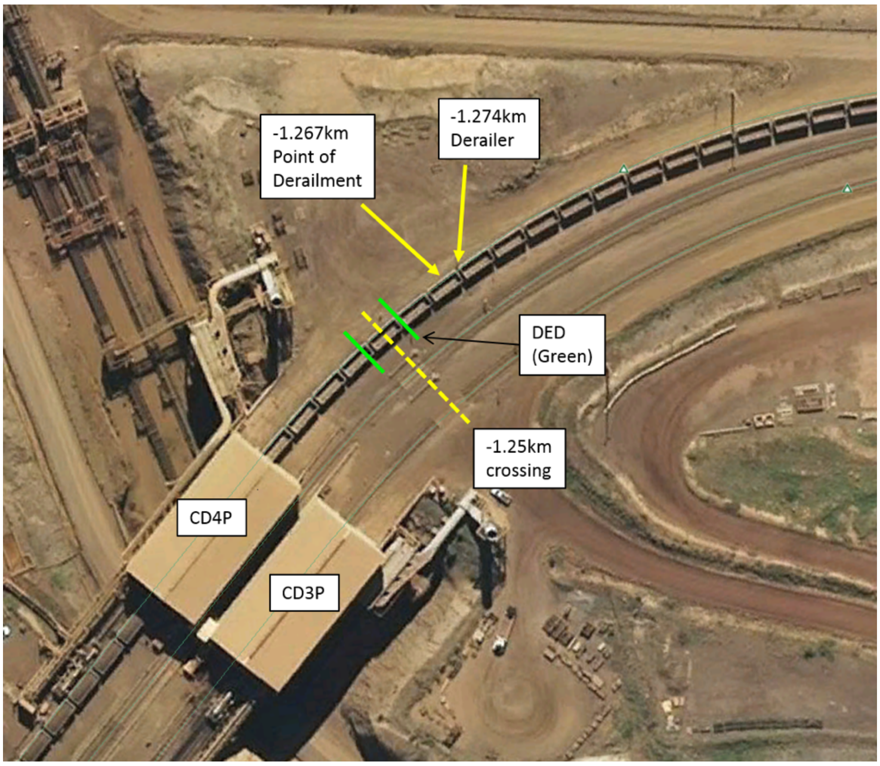


*Figure 15 Aerial layout of CD3P and CD4P*

## 3.3 Typical consist composition

Trains typically consist of 236 wagons, consisting of a mix of Q series and B series wagons. Each wagon is 9.3m long and 3.3m wide, giving a total consist length including draw gear of approximately 2300m. During the dumping process the mainline locomotives are uncoupled from the wagons and a break car is attached to the consist to enable controlled movement of the consist by the dumper indexing arm.

## 3.4 Track Design

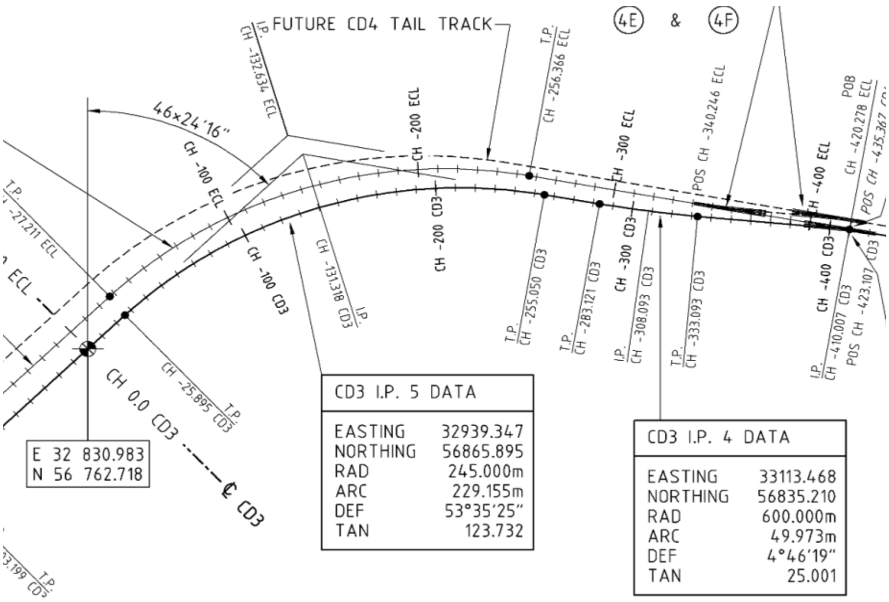


*Figure 16: Parker Point dumpers track profile.*

It should also be noted that the CD3 and CD4 empty car line horizontal curves do not have a transition spiral to ease rolling stock into the bend which may have helped the situation due to the wagons being propelled instead of pulled by the positioner arm. However according to the requirements laid out in DC-R001 Railway Route Infrastructure – Civil & Track, it is not required and there is a lack of space to install one.

Track geometry for yards and workshop areas, according to the current version of DC-R001, Railway Route and Infrastructure – Track and Civil are:

- Minimum horizontal radius of 300m desirable, with a 250m radius absolute minimum.
- Transition spirals are generally not provided.
- Maximum gradient of 0.1%.

## 3.5 Human factors

There is no evidence of fatigue, human error or other factors influencing any key personnel who were involved in the derailment. After the train is set in the dumper the process is automated.

## 3.6 Track Condition

All sleepers and fasteners were in good condition. The ballast was heavily contaminated with ore in the location however there was no evidence of significant movement of the track under load.

*Figure 17: Contaminated Ballast*

## 3.7 Track Geometry

The most important factor for the check rail was discovered from both eye witness derailment reports and site specific measurement and verification. The location where the concrete pad transitions to the earth laid sleepers creates a section of rapid modulus change. The addition of water to this area creates a situation where the soil elastic modulus is reduced and the continued weight of the wagon consists generates a dip. Continuous poor maintenance practice including wash-off, poor drainage and water run off also contributes to the dip in the track. This decreases the vertical force on the check rail and subsequently the ability of the check rail to resist lateral movement.

On the 6th of March 2016 It was measured that a 'dip' in the tracks was also evident. This dip was found as part of a derailment investigation and is assumed to be another factor in the derailments. The location of the dip is located just prior to the suspected point of the most derailment. This dip combined with small radius and no transition curve causes wagons to experience higher lateral forces at both the CD3 and CD4 outgo tracks.

The geometry defect is believed to be created by a combination of fouled ballast and water run-off from the dumper. The dip in the track has been recorded historically and despite previous rectification, the combination of continued washing down, poor drainage, combined with inadequate transition stiffness at the end of the concrete slab, caused the track to subside outside CD3P.

The below table shows the track dip measurements for CD3 tail track high leg with respect to the derailment location (0m). The 50mm laser height measurements indicate where the laser origin was at the time of measurement.

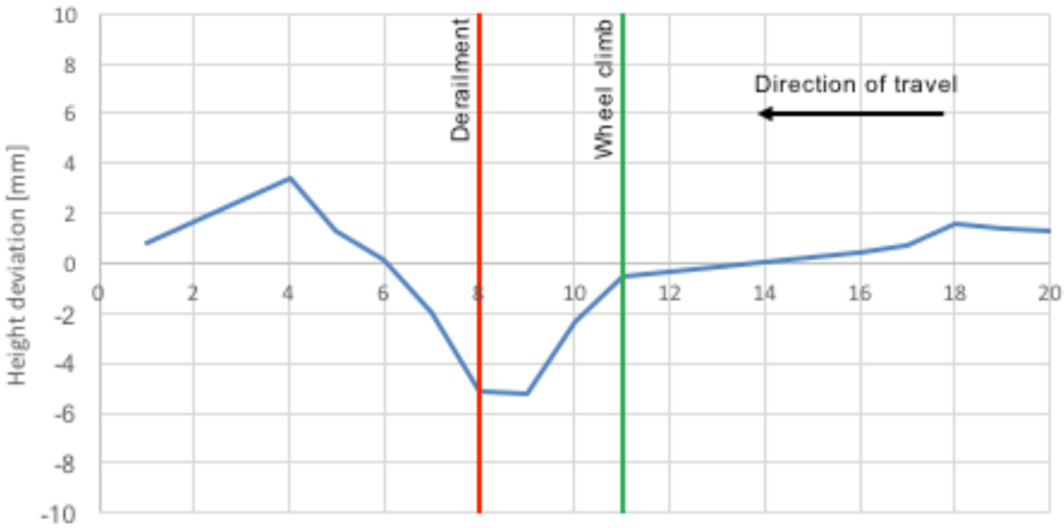


*Figure 18 Deviation of rail height with respect to averaged gradient*

*Figure 19: Evidence of Dip in Track*

## 3.8 Track Measurement

Measurements were taken of the gauge and superelevation along CD4P on 28th June 2016. Measurements started from approximately 600mm back from the edge of the concrete apron and went north to the crossing.

| Measurement | Superelevation | Track gauge |
|---|---|---|
| 1 | 7 | 1441 |
| 2 | 6 | 1441.5 |
| 3 | 6 | 1440 |
| 4 | 6.5 | 1439 |
| 5 | 5 | 1440.5 |
| 6 | 6 | 1442 |
| 7 | 7 | 1440 |
| 8 | 7 | 1439 |
| 9 | 6 | 1438.5 |
| 10 | 5 | 1439 |
| 11 | 6 | 1440 |
| 12 | 6 | 1439 |
| 13 | 6.5 | 1439 |
| 14 | 8 | 1439 |
| 15 | 9 | 1442.5 |
| 16 | 8 | 1444 |
| 17 | 8 | 1445 |

## 3.9 Radius of outgoing curve

Actual measurements determined the radius to be 245m on average with a minimum radius of 208m. The curve radius for CD3P empty car track, outgo side, was designed to be below the minimum radius stated in RTIO's Rail Design Criteria.

| Distance (m) | Versine (m) | Radius (m) |
|---:|---:|---:|
| 1 | 0.060 | 208.33 |
| 2 | 0.058 | 215.52 |
| 3 | 0.055 | 227.27 |
| 4 | 0.053 | 235.85 |
| 5 | 0.050 | 250.00 |

| | | |
|---|---|---|
| 6 | 0.050 | 250.00 |
| 7 | 0.052 | 240.38 |
| 8 | 0.054 | 231.48 |
| 9 | 0.055 | 227.27 |
| 10 | 0.056 | 223.21 |
| 11 | 0.058 | 215.52 |
| 12 | 0.058 | 215.52 |
| 13 | 0.056 | 223.21 |
| 14 | 0.055 | 227.27 |
| (end concrete) 15 | 0.050 | 250.00 |
| 16 | 0.045 | 277.78 |
| 17 | 0.042 | 297.62 |
| 18 | 0.040 | 312.50 |
| 19 | 0.042 | 297.62 |
| 20 | 0.046 | 271.74 |
| 21 | 0.050 | 250.00 |

## 3.10 Rail profile measurement

The rail profiles were measured using a Miniprof instrument at 2m increments, starting 16m back from the concrete apron. The profiles are shown in Figure 18, with the high rail profiles on the left side, and the low rail profiles on the right. The datum point for these profiles was the southern side of the IRJ, and the transition from the apron to the sleepered track was at the 18.5m position from this datum, corresponding to the edge of the concrete apron. Little wear was evident in the high rail up to the weld. Beyond this weld, the high rail exhibited significantly more gauge face wear; however, this was well beyond the relevant region where the wheel climbed the high rail. The low rail profile in the region of the derailment seems to be quite heavily worn, given that the traffic consists of slow moving empty wagons; this may indicate heavy loading in the region related to the vertical dip, but is not considered directly causal to the derailment.

The gauge width was extracted from the MiniProf profiles. According to these measurements, the gauge was well controlled on the concrete apron, at a value of 1435mm, but significantly increased at the transition from the apron to the sleepered track. The gauge width returned to a lower value beyond this transition region, but gradually increased along the curve, with another jump around the transition from the re-railed region at about 32m from the datum point, with the more heavily side worn rail exhibiting a gauge width with an average value of 1445mm.

The track at CD4P goes from tangent through the dumper to a relatively tight curve (av. 245m radius), with no spiral transition. This curve starts at the dumper area, but the region beyond the dumper apron is also considered critical as the steering of bogies under empty wagons is not good, such that the wheels would tend to flange heavily at the start of this curve.

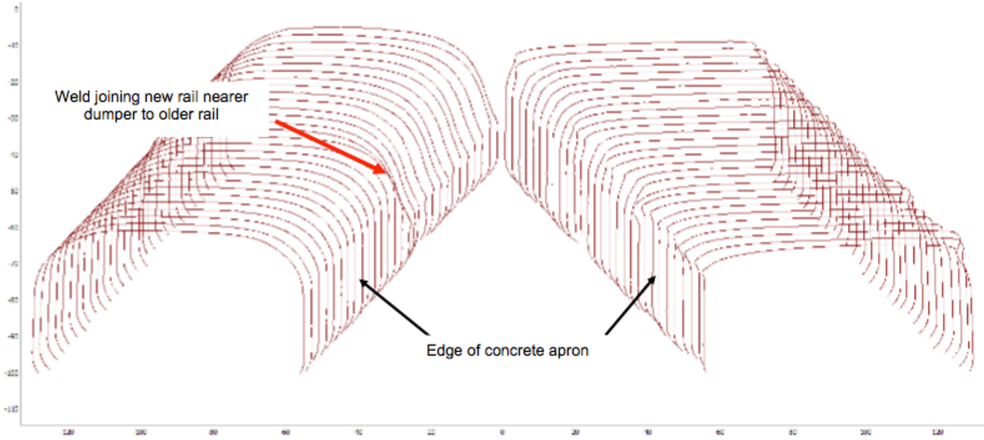


*Figure 20 The below tables are track dip measurements for CD4 tail track high leg with respect to the derailment location (0m). The 50mm laser height measurements indicate where the laser origin was at the time of measurement.*

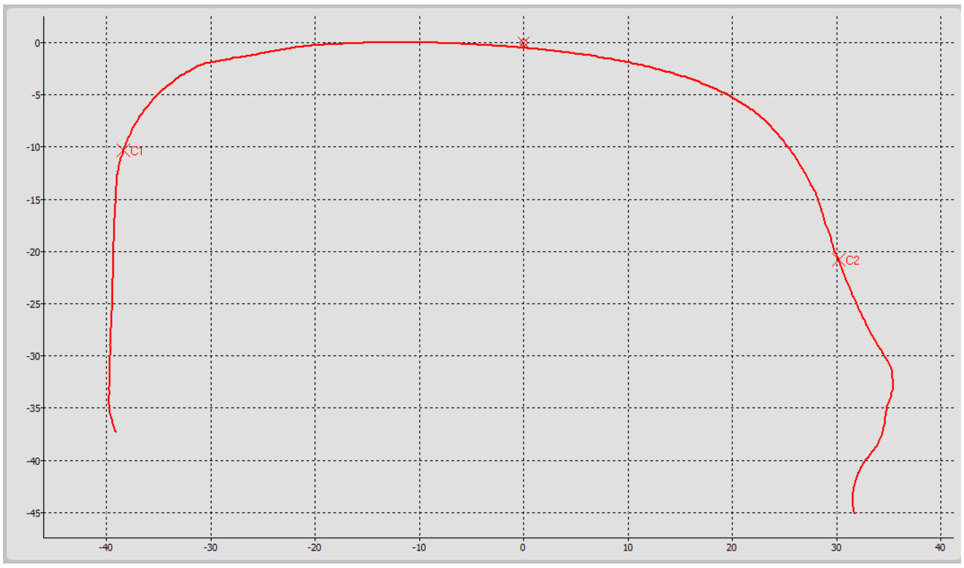


*Figure 21 High Leg track profile at point of climb initiation*

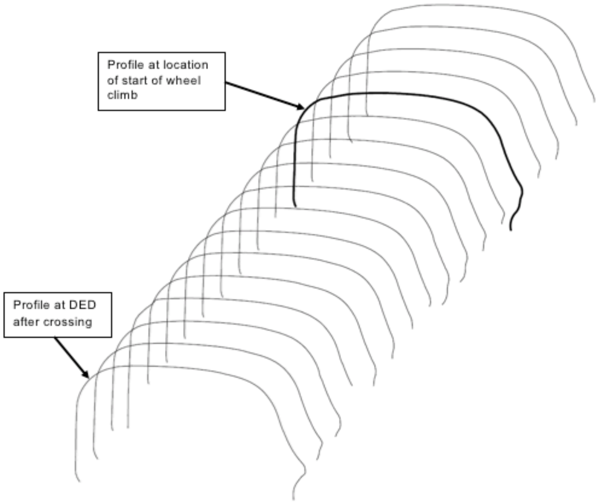


*Figure 22 Figure 5.4 High Leg track profiles in 1m intervals*

## 3.11 Existing Checkrail

The check rail itself consists of a number of 200mm wide brackets fixed to the sleeper with chemical anchors. Bolted to the top of the brackets is 125x125x16 even angle. There is approximately 30 metres of check rail outside each car dumper. Each 30m run of check rail is made up of three lengths of angle iron. The face of current check rail sits 105mm from the gauge face of the rail along most of its length. Outside CD3P this increases to 115mm for several metres. The brackets hold the check rail to roughly the same curve radius as the rail.

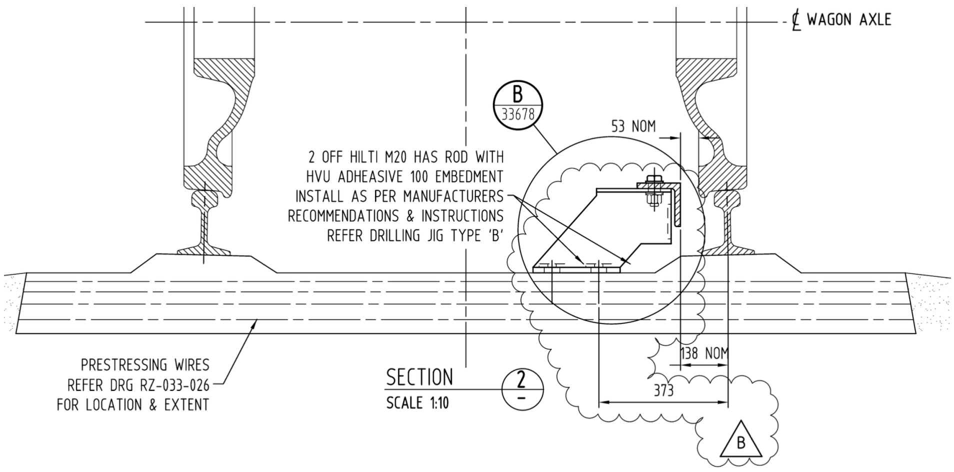


*Figure 23 Existing checkrail layout*

A review of the gap between the gauge face of the rail and the check rail at CD3P and CD4P was undertaken. The gap of the existing checkrail allows for the wheel of the wagon to have travelled past the centre point on the head of the rail before having any impact

## 3.12 Wheel profiles

Wheel tread readings were recorded by the OCCM system on the 27/06/16 and 18/07/16 for wagons B20270 and B20045 respectively and are as follows:

B20270 OCCM data

| Units in mm | Flange Thickness (Limit = 26.5 Minimum) | | Tread Thickness (Limit = 27 Minimum) | | Tread Hollowness (Limit = 2.4 Maximum) | |
|---|---|---|---|---|---|---|
| | Left | Right | Left | Right | Left | Right |
| Axle 1 | 33.3 | 34.6 | 41 | 42 | 0.8 | -1.0 |
| Axle 2 | 37.1 | 33.1 | 41 | 42 | -0.5 | 1.1 |
| Axle 3 | 33.7 | 34.2 | 42 | 42 | -0.6 | -1.1 |
| Axle 4 | 36.6 | 33.8 | 41 | 42 | -1.7 | 1.1 |
| Axle 5 | 33.0 | 33.8 | 41 | 42 | 0.6 | -1.5 |
| Axle 6 | 35.7 | 33.0 | 41 | 42 | -0.3 | 0.9 |
| Axle 7 | 33.9 | 34.6 | 41 | 41 | 0.9 | -0.9 |
| Axle 8 | 30.1 | 27.8 | 39 | 39 | -2.2 | -1.5 |

B20045 OCCM data

| Units in mm | Flange Thickness (Limit = 26.5 Minimum) | | Tread Thickness (Limit = 27 Minimum) | | Tread Hollowness (Limit = 2.4 Maximum) | |
|---|---|---|---|---|---|---|
| | Left | Right | Left | Right | Left | Right |
| Axle 1 | 31.9 | 30.0 | 40 | 40 | -1.8 | -1.6 |
| Axle 2 | 32.5 | 31.2 | 39 | 39 | -1.8 | -1.5 |
| Axle 3 | 32.8 | 31.5 | 39 | 38 | -1.6 | -1.6 |
| Axle 4 | 32.7 | 30.5 | 39 | 39 | -1.8 | -1.5 |
| Axle 5 | 32.4 | 30.4 | 39 | 39 | -1.6 | -1.6 |
| Axle 6 | 32.6 | 31.3 | 38 | 37 | -1.8 | -1.4 |
| Axle 7 | 32.9 | 30.8 | 38 | 38 | -1.7 | -1.6 |
| Axle 8 | 32.1 | 30.4 | 39 | 39 | -1.8 | -1.5 |

Note for above tables, wheel on high leg side of derailed wheel set is highlighted bold.
Once B20270 had been shunted into 7 Mile RSM for maintenance, the wheel profiles were measured. Unfortunately, B20045 was missed. Figure 21 shows the profile of wheel R1 of wagon B25270 – the wheel that climbed the high leg of the rail.

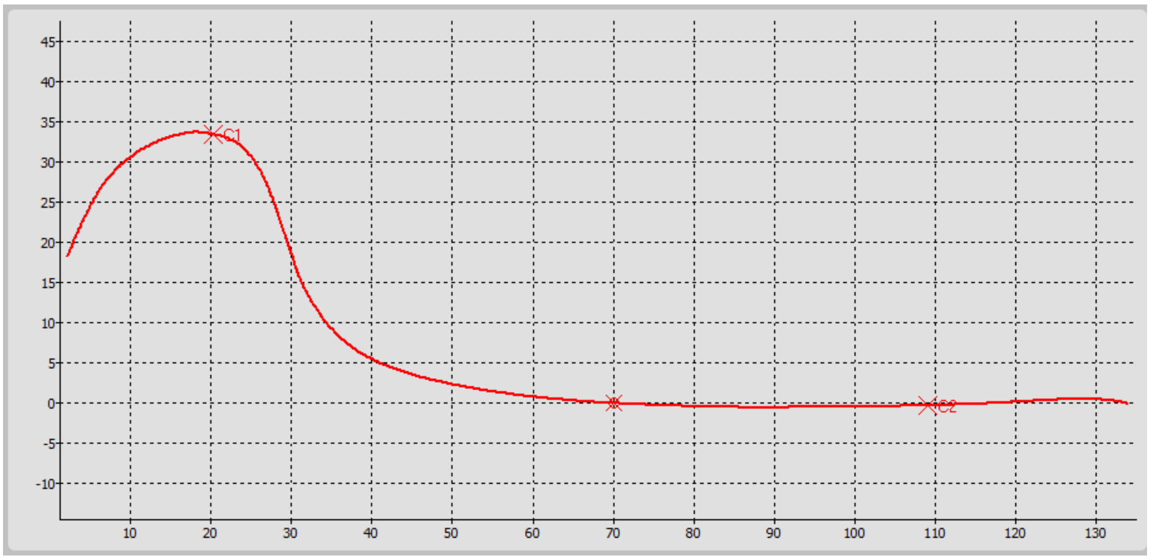


*Figure 24 Wheel profile of B20270's derailing wheel (R1)*

## 3.13 Vehicle types and alignment

Maintenance History of wagon (B20270)

Wagons B20270 and B25270 were commissioned on the 1/08/2014.

B20270 Maintenance Activity

| Action | Planned | Status | External Id | Priority | Raised | Completed | Description | Axle | Side | Wheel Number |
|---|---|---|---|---|---|---|---|---|---|---|
| Notification | No | Pending | 26486722 | 90 | 14/10/2015 | | Replace End Cock and Extension Handle | - | - | - |
| Notification | Yes | Pending | 28320531 | 50 | 10/02/2016 | | 20270 Wagon/ECP Service | - | - | - |
| Notification | No | Completed | 28458501 | 10 | 21/02/2016 | 10/03/2016 | Hot wheel | - | - | - |
| Notification | No | Completed | 28608990 | 10 | 10/03/2016 | 10/03/2016 | Replace fixed knuckle | - | - | - |
| Notification | No | Pending | 29465898 | 10 | 29/06/2016 | | Derailed Wagon Requires inspection by RE | - | - | - |
| Wagon Pair Major Service | Yes | Completed | 19258286/0010 | 50 | 30/06/2016 | 30/06/2016 | B Series Wagon 2Yr Service | - | - | - |
| Wheelset | No | Completed | 28560194 | 30 | 4/03/2016 | 10/03/2016 | Multiple B WID alarms - R8 | 8 | | |

Hide deleted

*B20270 maintenance history*

This wagon pair completed a 2-year service on 30/06/16 after the post-derailment inspection, just over 1 month early. There were no reports of misalignment of any components or irregularities

Maintenance History (B20045)

Wagons B20045 and B25045 were commissioned on the 17/09/2013.

B20045 Maintenance Activity

| Action | Planned | Status | External Id | Priority | Raised | Completed | Description | Axle | Side | Wheel Number |
|---|---|---|---|---|---|---|---|---|---|---|
| Notification | No | Completed | 29183354 | 10 | 23/05/2016 | 22/05/2016 | ECP fault CCD U/S | - | - | - |
| Wagon Pair Major Service | Yes | Completed | 18169073/0010 | 50 | 1/07/2016 | 2/07/2016 | B Series Wagon 2Yr Service | - | - | - |
| Notification | No | Pending | 29476268 | 10 | 30/06/2016 | | Derailed Wagon Inspection | - | - | - |
| Notification | Yes | Completed | 24981917 | 10 | 2/07/2016 | 2/07/2016 | 20045 Wagon/ECP Service | - | - | - |
| Wheelset | No | Completed | 29183352 | 10 | 23/05/2016 | 22/05/2016 | WID L1 | 1 | | |

Hide deleted

*B20045 Maintenance History*

This wagon pair underwent their 2-year service on 1/07/2016 after the post-derailment inspection, 9.5 months overdue. Wheel set 1 was replaced on the 22/05/16, just over a month before derailment. There were no reports of misalignment of any components or irregularities and the wagon was in service.
Visual observation and site accounts indicate that the wheel set of B25270 underwent a twist around the high leg rail which lifted the low leg side wheel approximately 20mm.

## 3.14 In Train Forces

The dumper positioner arm is controlled by 13 variable voltage/variable frequency (VVVF) drives. These drives are controlled by a PLC that controls the positioner arm movement against torque, speed and acceleration limits. It also logs the positioner arms location and the torque the drivers are producing at a 1 hertz frequency.
The CITEC dumper profiles were analysed for the minimum, maximum and average for both torque and speed for each of the 13 motors and nothing indicated abnormal operation. the positioner arm showing an average torque of 341.4 Nm for the motors. This is not an unusually high torque for the dumper.

IOC data taken from the few months before derailment shows a ramping up of in train compressive forces during approximately the last 30 wagons. The figure below shows an overlay of 3 separate IOC trips through the dumper with varying position within the consist. The overlay shows that the compressive forces can ramp up to 80 tonnes compressive force.

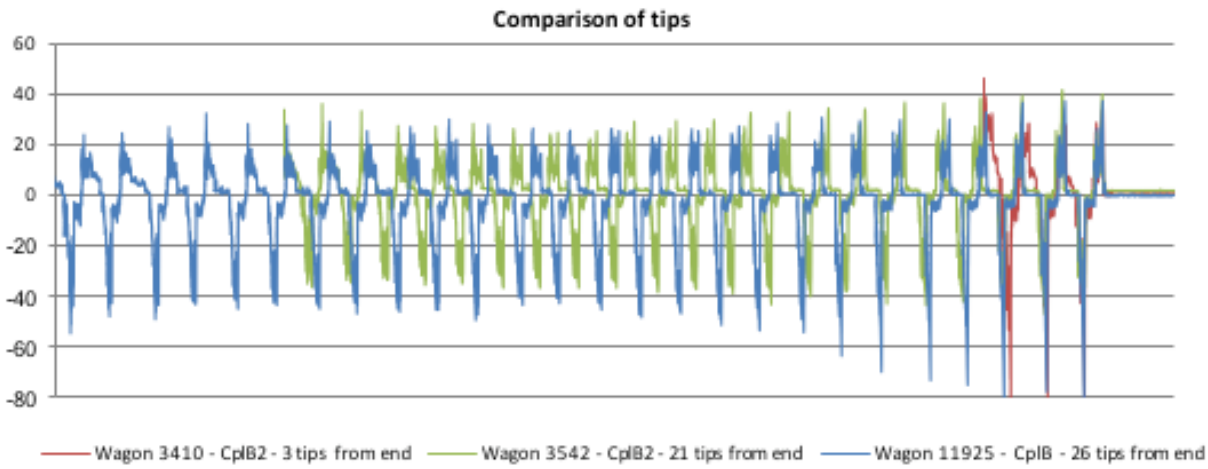


*Figure 25 Overlay of in-train forces during dumping of last wagons*

## 3.15 Coupler Forces

A brief review of coupler forces was performed on the data from the IOC wagons, and found that the coupler forces acting on the empty ore wagons during the indexing cycle were quite variable, and can be very large. In the recent data from IOCs that transited CD4P in the past two months, there were 18 runs from 11 IOCs that were within 10 pairs from the end of a tag. These identified that the compressive loads increase gradually to a maximum value as the wagons ahead are pushed by those nearer the exit of the dumper. The peak loads varied from about -40 tonnes (IOC 3934) force to a maximum of -100 tonnes (IOC 30301) force, where IOC 3934 was within 7 pairs and IOC 30301 was within 3 pairs from the end of the tag respectively.

# Chapter 4 RESULTS AND DISCUSSION

Review of existing conditions indicates that there are multiple possible contributing factors to the flange climb derailments.

## 4.1 Risk assessment

### 4.1.1 Safety in Design

The design of this check rail in line with the requirements of Regulation 3.140 of division 12 of the Occupational Health and Safety Regulations 1996 outlines the design risk and identifies:

- The hazards identified as part of the design process that arise from the design of the end product, or to which a person at the construction site would be exposed;
- The designer's assessment of the risk of injury or harm resulting from those hazards;
- The designer's action taken to reduce those risks;
- Any parts of the design where hazards have been identified but not resolved.

The risk assessment shown in appendix C, identifies the hazards that are considered of a non-standard nature, unusual, specific to the design or otherwise noteworthy. Risks such as working at heights, slips/trips and working around live rail are examples of risks considered standard.

## 4.12 Consequential effects and ethics

Development of a custom and fit for purpose design, followed by effective implementation will improve the sustainability and efficiency of the RTIO rail network and will reduce downtime. The ability to reduce the hazards created by derailment will improve the safety for all personnel working on and near the car dumpers. Given the number of derailments occurring on the area, it is imperative that this project assesses all aspects associated with the derailments and does not overlook the contributing underlying causes, including track geometry, rail wear and rolling stock interface. The pressures associated with implementing a design on an active rail network generally dictate that the solution will be implemented quickly with minimal track closure. The pressures to complete the installation in a minimal timeframe can lead to compromised design and may ultimately lead to the installation of an ineffective solution. The installation of an ineffective solution is not only a waste of money but also maintains or reduces the safety of the network. This project will deliver an effective and fit for purpose design with due regard for the constructability of the solution, ensuring an optimal outcome.

## 4.13 Track Condition

The high rail of the outgo track was measured using the MiniProf Rail device and, while visually deformed, was found to be within Rail Division's standards for rail wear. The Track and Civil Code of Practice (Vol 1 – Rail) outlines the maximum allowable head loss for curves less than 1000m as 35% (area), the figure below indicates the rail was within these limits.

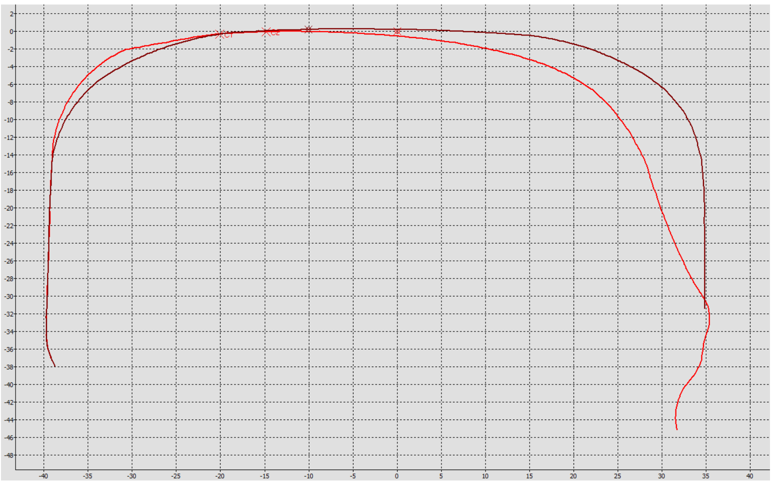

*Figure 26 Figure 6.1 CD4P outgo high rail (red) and new rail (dark red) profiles*

The side wear measured is also within the Code of Practice's limit of 10mm, reaching a maximum of around 8mm. The track limits are set in the code of practise and the track is passed and failed by the inspectors against these limits. This being said, the rail head wear limits are designed to prevent fatigue related rail failures only and do not consider wheel/rail steering interface (this may have an influence on the limits but the main objective is to reduce the risk of rail failures). Therefore, while the high leg rail of the CD4P outgo curve may be within rail wear limits, the profile is not measured against criteria for wheel interaction which will leave the elevated derailment risk unnoticed in the current maintenance systems.

The high rail of the tail track had a severely worn gauge face which enabled a lower contact angle between rail face and wheel, leading to derailment through flange climb.

The 'lip' that had developed on the gauge face creates a shallow wheel/rail contact angle. Once the wheel is pushed high enough, the lateral force required to continue the flange climb is much lower than with a standard rail profile. The below figure demonstrates the interaction between the derailed wheel profile at the point of derailment for wagon B25270. The second derailed wagon, B25045, was not recorded with the wheel MiniProf.

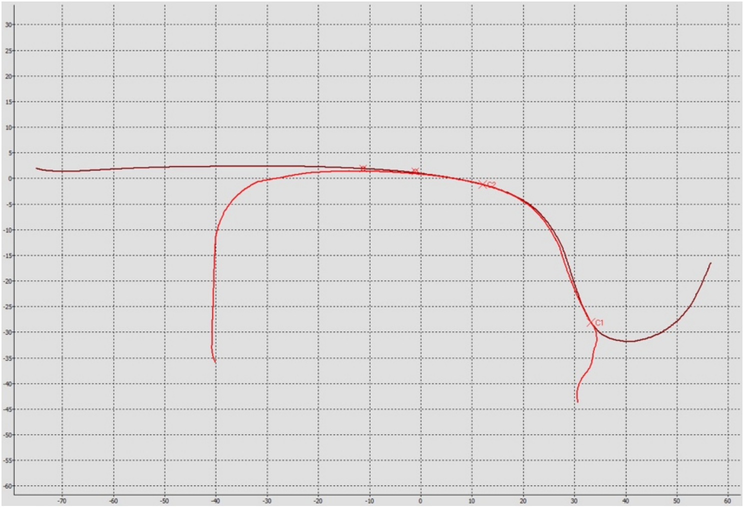

*Figure 27 Wheel and rail profiles at location derailment*

Once the wheel is hard against the flange (similar to the above figure) the gauge face 'lip' can contact the wheel's flange (if the flange is high enough) allowing the wheel to ride up onto the lip due to the lower contact angle. The wheel will then only have the desired steep contact angle with the rail head for a short vertical distance which greatly increases the chance of derailment. The wheel will be more susceptible to short periods of high lateral force pushing it out of the rail. For comparison, the figure below shows the contact the derailed wheel would have had with a section of new rail. Note the contact angle is much steeper at the wheel/rail contact point and will stay steep for a large portion of the possible derailment path.

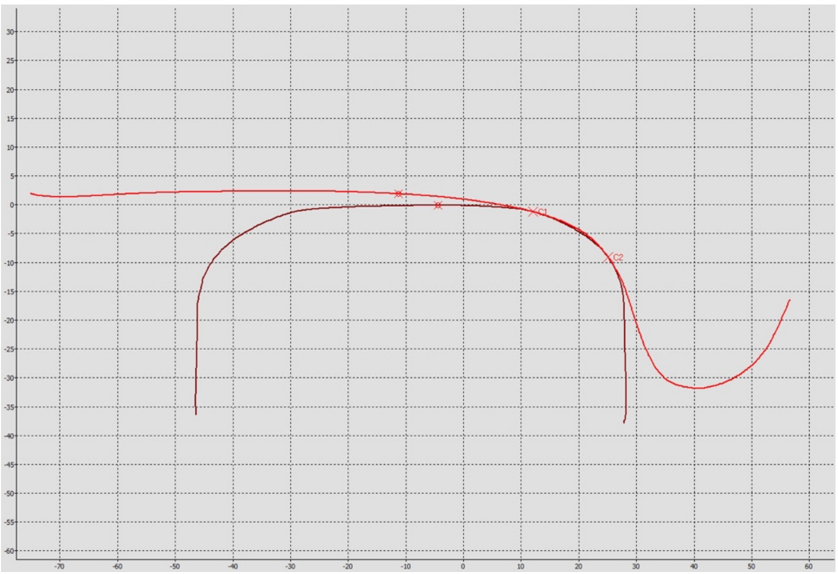

*Figure 28 Wheel with new rail profile*

It is suspected that due to the severely worn profile of the high rail, a rail with the profile of a new rail would have greatly reduced the risk of derailment along the curve due to the steeper contact angle.

## 4.14 Track Dip

The measured dip in the track was small enough in this instance that it was not considered to be a contributing factor on its own, however the addition of high in train forces from the dumper indexing arm is viewed as significant. The dip depth of 10mm over 4m is outside of the class A track target Geometry limits but falls within the defect limit. The fact that the wheel started climbing on a section without a large change in rail height indicated that the track geometry had little to no influence on the cause of the latest derailment on this single occasion. This should not discount the fact that this issue requires rectification.

## 4.15 Wheel profile

The measured wheel profile does not appear to be a factor in the derailments. The wheel set condition of both wagons that derailed during the 28 and 29 July derailments is not considered to be a contributing factor for the derailments. The wheel profiles of all the wheels of wagon pair B20270/B25270 were measured using the Wheel Miniprof.

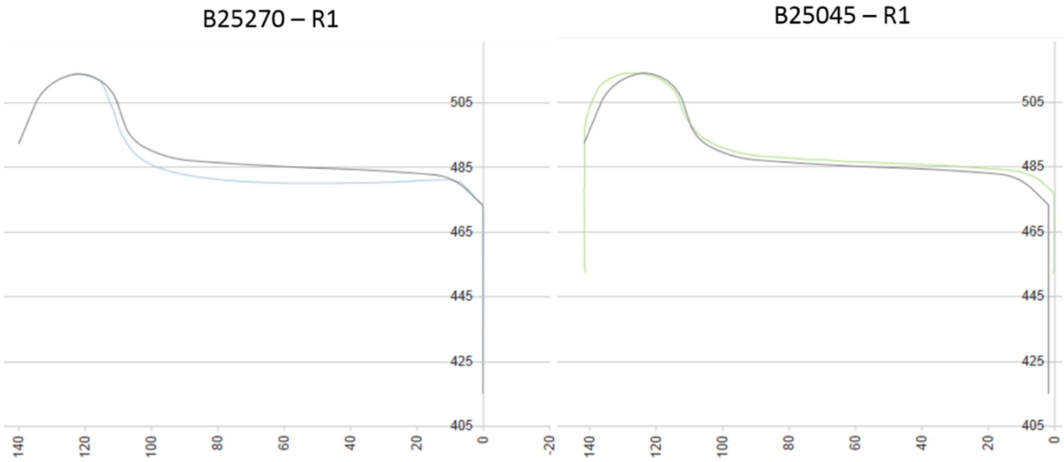


*Figure 29 Derailed wheel profiles (Black is new wheel)*

OCCM wheel profiles were available for both. All OCCM measurements were within shop limits in accordance with Rolling Stock Shop Standards and the Standard for Qualifying Wheel Sets. There were no obvious errors in wheel profiles for both derailed wheel sets. The derailed wheel set on wagon B25270, although still within limits, had slightly shallow wheels:  The wheels on each occasion are within the design tolerances and are regularly maintained to a sufficient standard. Flat wheels and defective wheels are identified by asset protection devices and have not been identified

*Figure 30 Using the AAR Wheel Gauge to measure wheel flange height (left) and thickness (right)*

## 4.16 In train force data analysis

The risk of derailments increases substantially under the combination of high lateral loads and reduced vertical loads. While the reduction of dumper torque would certainly help, this comes with a substantial economic penalty, as it would tend to increase the cycle time for dumping. On a cumulative basis, this is significant, and would become more so in the absence of realignment.

Instrumented Ore Car in-train force readings indicate a large increase in compressive forces during indexing the last 30 or so wagons, leading to a larger lateral force applied to wheels along the CD4 and CD3 tail track curve. This force has been measured (pre-derailment) to be upwards of 80 tonnes, whereas the general compressive force during the rest of the dumping cycle averages around 45 tonnes.

The presence of a dip can lead to substantial unloading of wheels, due to the high forces, as the coupler connection to the wagon ahead can support a large vertical load in addition to the horizontal load. This is much more likely when there are high compressive longitudinal forces present at the indexing arm and possible brake stick.

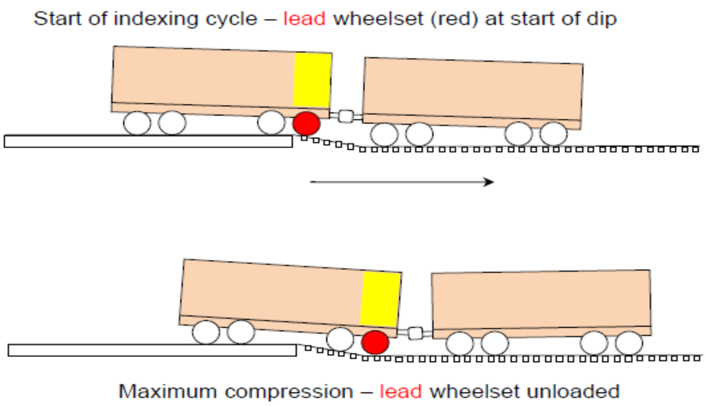


*Figure 31 Indexing cycle*

## 4.17 Calculate lateral forces

The track layout in this area has been discussed with a key feature of the tracks from both dumpers is that they are on relatively tight curves of less than 250m. The curves start just inside the dumper buildings. This layout was unavoidable given the location of these dumpers, but means that these locations are particularly prone to high lateral loads due to the curvature of the track towards the high rail leg. In effect, the ore wagons can be considered as a long column, which is prone to buckling instability if it is insufficiently constrained under compressive loads.

Derailments where the wagons were being indexed at the time generally occur at the same location just clear of the concrete apron on the outgo side. It can be seen that the derailments while being propelled by locos occur within the first curve but may be further from the dumper.

When propelling a consist of wagons on flat or uphill alignment through curves, the frictional resistance of the preceding cars increases the lateral force applied to cars located closer to the locomotive or indexing arm.

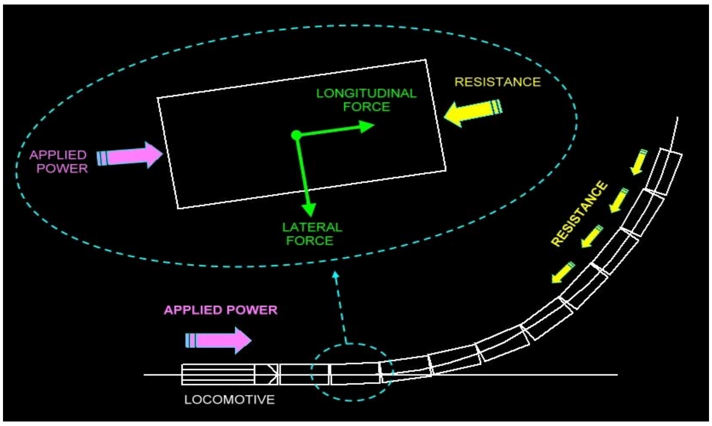


*Figure 32 Lateral force due to resistance of wagons*

Hence, it is not always the leading cars that derail, but cars closer to the locomotive or indexing arm.

The resistance is highest in tight curve situations, with dry unlubricated rails and freshly machined wheels. The lateral force vs. vertical force ratio (L/V) is often used as an indicator of adverse rail-wheel contact conditions that can lead to flange climb as governed by the Nadal equation.

The main variable in this situation (given geometric conditions) is friction, and by controlling the adhesion levels at the rail-wheel interface it is possible to control the creep forces and hence L/V ratio of the vehicles.

Creep forces and hunting are reduced in cases of wet rail or modified (lower) adhesion levels. Hence it seems less likely that derailments would have occurred when rails were wet. Adhesion levels vary considerably due to environmental factors and the condition of the wheel and rail surfaces in contact.

Tribometer instruments can be used to measure adhesion levels at slow speed, walking pace. In this process brakes are applied to a measuring wheel with controlled loading which defines the limiting adhesion as the wheel begins to stall/slip. Typically, top of rail values, without lubricant contamination, deliver friction values ($\mu$) in the 0.4-0.5 range. These instruments tend to saturate at ~0.6, such as for freshly ground rails.

Under normal operating conditions the values outside of the dumpers is measured at ~0.5 or less. It is often determined that, with speeds of 5-15km/h, the wagons will retain higher adhesion levels and hence develop higher lateral forces and L/V ratios. Lateral forces

The track design radius of the PPCD4TAIL curve is below the recommended absolute minimum radius specified in Railway Route Infrastructure – Civil & Track engineering standard (DC-R001). Section 10.9 of the standard states a "minimum horizontal radius of 300m, with a 250m radius absolute minimum. Transition spirals are generally not provided". The design track radius of the CD4 (and CD3) tail tracks are 245m, where the actual radius was measured to be less than this value.

The higher the lateral forces applied to the wheel/rail interaction, the higher the chances of derailment. In this situation the lateral forces cannot be reduced through increasing the track radius so must be controlled through the reduction of in-train forces.

The two components of in-train forces along this curve are:

- The force exerted by the positioner arm indexing the consist forward, and;
- The resistance from pushing the rest of the consist.

This resistance is a combination of rolling resistance (wheels interacting with the rail, friction in bearings, etc.) and inertia (moving a body from rest). Both are largely unchangeable, although good wheel and rail profiles will help reduce this resistance.

## 4.18 Friction control

It can be seen that the absence of lubrication and friction control results in highly variable conditions depending on the action of wheels ahead of wagons that derail. The freshly machined wheels that scrape and clean the rail, lift the effective adhesion due to the machined face and tight radius. The Nadal formula, defining the required L/V ratio to satisfy wheel climb is simplistic yet indicative of the primary requirements. It incorporates

the contact or flange angle and the adhesion level. It can be shown that a lubricated rail offers greater resistance to climb as does a steeper flange angle. Hence the greater resistance to start a wheel climb reduces as the wheel moves on to the gauge corner or tread and onto a flat surface.
The saving grace in these cases is the much larger rolling radius at the flange that provides a strong restoring effect by trying to steer the wheelset back onto track.

High adhesion limits such as those that occur with the cleaning action of machined wheels, reduce the safety margin where wheel unloading or wheel lift become more effective in starting and maintaining wheel climb.
The L/V ratios of ~0.5 in 230m radius curves apply to standard wheel profiles corresponding to new wheels entering service. Worn-in wheels, fare better with lower L/V ratios, other factors being the same. Worn bogies with a degree of wear/slop in the damping system, whilst less desirable for mainline, tend to curve more favorably and are less likely to climb the rail. An extrapolation of these results to higher adhesion limits would increase L/V ratios to the point where they would satisfy the basic requirements for wheel climb. Consequently, the inability to screen rolling stock for the right of passage, requires friction modifiers and lubricants to raise the overall insurance level and resist wheel climb derailments.

Friction modifiers typically try to stabilize adhesion at ~0.3 and would offer some improvement in derailment resistance. In addition, rail gauge face/flange lubrication would be required to increase the safety margin. Given that 0.2 friction levels are realistic, then a doubling of the L/V threshold would be achievable.

## 4.19 Changes to dumper and track

In 2007 and again in 2015 a positioner torque limit was applied to reduce the amount of compression pushed into the train. A train brake pipe gradient limit was applied to limit the potential brake application.
Post 2009 derailments a more conservative positioner torque limit (500Nm) was implemented for the last 40 cars of the train. More sophisticated limits were implemented for brake pipe pressures and gradients to detect possible sticky brake events. Post 2010 derailments the heavily worn rails at the CD3P outgo were replaced. The check rail was installed early 2013 and the existing DED moved from just clear of the concrete apron to just before the level crossing and an additional DED installed after the crossing. A re-railer was also installed after the first curve.

Prior to 2013, derailments that occurred during indexing, occurred immediately after the DED and often were not detected until they caused a larger derailment. While the checkrail has not prevented derailments it has reduced the derailments from 2 or more wheelsets to 1 wheelset. The movement of the DED has significantly reduced the consequence.
Since the last derailment in June 2016 the implementation of new drainage at the end of the concrete apron as well as re-rail of the high leg has been undertaken

## 4.1 Applying Nadal limits to current check rail design

Since derailments have occurred at the CD3P and CD4P dumpers, the Nadal equation can be used to estimate the minimum lateral force occurring to cause a derailment. The static coefficient of friction for steel on steel ranges from 0.5 to 0.8 depending on surface condition. For new wheels θ is approximately 72°. After machining this changes to 75° as Rio Tinto machine to AAR standards. These numbers give a lowest L/V as 0.6 with a friction factor of 0.8 but could be up to 1 if the friction factor is closer to 0.5. Hence the lateral force on the wagon could be equal to the vertical force from the 21000kg empty weight.

$$\left(\frac{L}{V}\right) = \frac{\tan(72) - 0.8}{1 + 0.8\times\tan(72)} = 0.657$$

$$L = 0.657\times V$$

It is important to note that the L/V ratio increases as theta increases or the coefficient of friction decreases. Hence for a lower coefficient of friction or greater contact angle ($0\leq\theta\leq 90$) the system can sustain higher lateral forces without derailment.

Originally the wheel set first climbs the face of the rail and then climbs the face of the check rail. Numbers can be applied to the Nadal equation to show the likely outcome of this situation. First the wheel climbing the rail will be examined. As this is a tight curve, it is assumed that the steel is well polished and a friction factor of 0.5 will be chosen. It is also assumed that each wheel set supports a quarter of the empty wagons 21,000kg mass. This means each wheel would have a vertical force of 2625kg (25.75kN).

$$\left(\frac{L}{V}\right) = \frac{\tan(\theta) - \mu}{1 + \mu\times\tan(\theta)} = \frac{\tan(72) - 0.5}{1 + 0.5\times\tan(72)} = 1.0153$$

$$L = 1.0153V = 1.0153\times 2625 = 2665.2\ [kg]$$

Hence the lateral force on the front wheel set must be at least 2665.2kg for the wheel to derail. Once the wheel has ridden up into the centre of the high rail, the check rail is struck. For the check rail it was shown that the approximate contact angle was still 72 degrees. Since the check rail is not struck regularly (from inspection) we will assume a friction factor of 0.8 for rusty steel.

$$\left(\frac{L}{V}\right) = \frac{\tan(\theta) - \mu}{1 + \mu\times\tan(\theta)} = \frac{\tan(72) - 0.8}{1 + 0.8\times\tan(72)} = 0.65788$$

$$L = 0.65788V = 0.65788\times2625 = 1726.935\ [kg]$$

Hence if we originally had 2665.2kg of lateral force or greater to cause flange climb and the same conditions are continuing, the check rail will only be able to withstand 1726.935kg of lateral force. Hence the wheel set will climb the check rail and derailment will not be prevented.

## 4.2 Assessment of current checkrail effectiveness

General assessment of the existing checkrail shows that it is ineffective in achieving its intended function in its current configuration. The fact that it has a gap is so large that it allows for the flange to have passed across the centre point of the head of the rail as well as the lack of bracketing and therefore potential for deflection causes the existing rail to be ineffective. The combination of these two factors reduces the check rails effectiveness far below the theoretical value. In this instance it is assumed that a 77% improvement that could have been achieved under ideal conditions. Assuming a 1:1 L/V ratio without the check rail, the moment would reduce the effective vertical force on the wheel.

It is important to note the possible disconnect between the improvement in lateral force resistance by alteration to the checkrail. The improvement in theoretical values and resistance to derailment and the improvement in derailment occurrence numbers is not necessarily guaranteed or directly correlated. For instance, if alterations to the check rail show that we can sustain 177% of the lateral force that the current design allows for but dumper events, however the force created at the dumper indexing arm, that cause a derailment are always 200% of the lateral force that the new checkrail design allows, there will be no reduction in derailments, despite the new design being 77% better than the old design. Further information is required regarding the indexing forces from the dumpers.

As well as rotating a bogie to determine flange way clearances, the bogie can be rotated to emulate a derailment. The positioning of the wheels and the bogie can then be found at the point that the check rail contacts the wheel during derailment. This is shown in “Figure 33: Contact on check rail during derailment (red)” below.

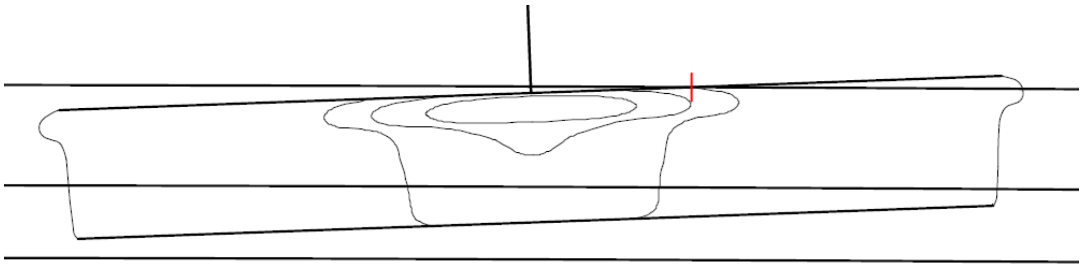

*Figure 33: Contact on check rail during derailment (red)*

Once this contact point is found, a slice can then be taken through the wheel to see what the cross-section of the wheel is at the contact point. From this cross section the contact angle can be calculated.

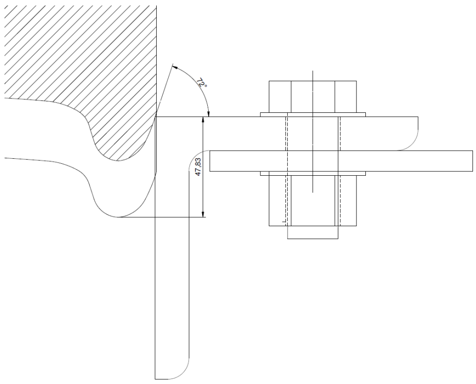

*Figure 34: Section View: Contact angle of wheel on check rail*

There are a couple of other factors that affect this number slightly, such as the wheel at the other end of the axle riding on the rail head (and thus changing the wheel set angle) and the horizontal and vertical deflection of the check rail. This diagram highlights why the current check rail often doesn't work. A wheel set derails on the outer rail with a certain lateral force as per the Nadal equation presented earlier. The outer wheel is already on the flat head of the rail before the inner wheel strikes the check rail. Re-applying the Nadal equation to the check rail, there is an equal or lower contact angle as well as likely a higher friction factor (due to the check rail being rusted and not polished like the rail surface). This means the check rail can sustain a lower lateral force then the external rail before flange climb derailment occurs. Hence if the force that begun the derailment continues for long enough, it will push the wheel set over the check rail as well. Once the first wheel set has been derailed, the angle of attack greatly increases. This lowers the contact angle (a 90-degree angle of attack would have a contact angle of about 36 degrees) and makes it easier for the other wheel sets to derail.

The efficiency of the check rail can be increased by moving the check rail in closer to the wagon wheel. This increases the lateral force needed to cause flange climb derailment as the outside wheel must climb the rail at the same time that the inside wheel is climbing the check rail. This increases the amount of vertical force available to push the bogie back down into its proper running position.

## 4.3 Limitations from Locomotive Wheel Base

The longer wheel base of the locomotives limits the amount that the check rail can be moved in closer to the gauge face of the rail. If the check rail is moved in too close the locomotive wheels will be "wedged" between the gauge face of the rail and the check rail. Nytram plots similar to those done for the wagon wheels suggest a 60mm gap would be appropriate. A decision may need to be made for construction tolerances although if it is only a small distance out, the check rail will likely wear into the ideal position.

Measurements were also taken using a camera underneath a stationary locomotive part way through the curve. This shows the locomotive in a static condition. It is difficult to use this method to come up with an accurate measurement as low image quality, perspective and the assumption that the check rail is straight all distort the values. Red lines show the original gap estimation and blue lines show a revised estimation. The revised lines would allow us to have a 65mm gap before the loco wheel touches the check rail. Measurements show 40mm between the check rail and the back of the loco wheel leaving 65mm of free space. What was not measured in the photo was the placement of the other wheel. This measurement should be repeated as accurately as possible prior to installing the check rail to verify design spacing from the drawings.

## 4.4 Deflection

In reality we are unlikely to see as big a benefit as identified for the mathematics due issues with both track condition and check rail design. The existing checkrail has up to a 2.36-meter gap between brackets. This large distance has the potential to allow the checkrail to deflect. It can be seen from previous calculations that if the check rail deflects 5mm (from 55mm to 60 mm) then our benefit drops from 77% over current case to 26%. It is likely the large gaps between the brackets will create a larger then 5mm deflection at points and hence the benefit of moving the check rail will vary between 77% better and no better along its length depending on the deflection.

## 4.5 Modification of existing check rail

For a 60mm gap the inside wheel contacts the check rail when the outside wheel is mid-way through climbing the high rail.

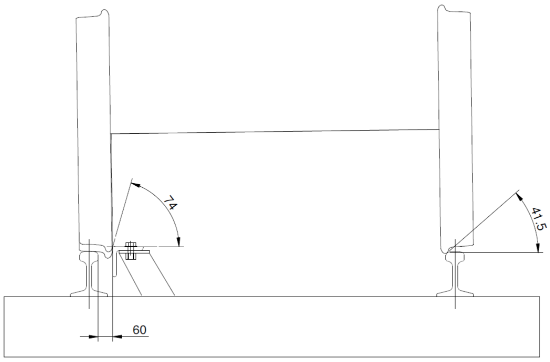


*Figure 35 Altered checkrail with 60mm gap*

It was shown from the Nytram diagrams that moving the check rail in to a 60mm gap would cause a 74-degree contact on the check rail. Again we will assume a friction factor of 0.5 for the rail and 0.8 for the check rail. The contact with the rail head was determined to be at 4.68mm in which corresponds to an angle of 41.5 degrees. It is also important to note that each wheel has a 2625 vertical force on it.

$$\left(\frac{L_1}{V}\right) = \frac{\tan(\theta) - \mu}{1 + \mu\times\tan(\theta)} = \frac{\tan(74) - 0.8}{1 + 0.8\times\tan(74)} = 0.7091$$

$$\left(\frac{L_2}{V}\right) = \frac{\tan(\theta) - \mu}{1 + \mu\times\tan(\theta)} = \frac{\tan(41.5) - 0.5}{1 + 0.5\times\tan(41)} = 0.2667$$

$$L = L_1 + L_2 = 0.9665V = 0.9758 * 2625 = 2561\ [kg]$$

This reflects the absolute worst case performance of the check rail due to geometry changes alone. This is only just lower (100kg) than the peak lateral force required to climb the rail head on its own. It is likely however that the check rail will have more frequent contact and this will polish the surface, lowering the friction factor.

## 4.6 Increasing the check rail height

Moving the contact point onto the flat at the back of the wheel would create a huge difference in the Nadal ratio. The obvious way to do this is to raise the check rail height. It is not possible to go above the height of the fixing however the fixing is more than 12mm above the height of the check rail. The Nadal ratio for an angle of 90 degrees is as follows:

$$\left(\frac{L}{V}\right) = \frac{\tan(\theta) - \mu}{1 + \mu\times\tan(\theta)} = \frac{\tan(90) - 0.8}{1 + 0.8\times\tan(90)} = 1.25$$

$$L = 1.444\times V = 1.444\times 2625 = 3790.5$$

If the coefficient of friction is taken at 0.5 the L/V ratio increases to 2. At first glance this is a large win however this effect is not actually realised. On closer inspection, as the check rail height is increased, the contact point moves up and out on the wheel. This leads to it still contacting on the curved surface on the outside of the wheel which creates the same 72-degree angle. It does however slightly increase the amount of time the lateral force must be applied to create a derailment.

## 4.7 Moving the contact face

The existing check rail can be moved by either manufacturing new sets of angle iron or facing the angle iron with steel plate. The contact surface should be moved to 60mm away from the gauge face of the rail. This gives a wear resistant surface that will give the improvements due to the geometry change. Hence facing the check rail with steel should give a low maintenance solution will give significant improvement to the lateral force resistance.
In addition, moving the contact surface should also halve the angle of attack. This will increase the climb distance required for derailment.

## 4.8 Checkrail Gap reduction

Should the gap between checkrail and stock rail be reduced for a 60mm gap, the geometry and the action of the checkrail will change. The change will cause the inside wheel to contact the check rail when the outside wheel is mid-way through climbing the high rail. The distance between the check rail and the gauge face of the rail allows the wheel to first ride over the high rail and then ride over the check rail. While this does increase the time personnel have to react before a severe derailment occurs, it does not reduce the number of incidents. Theoretically, the check rail should be moved so that the wheels must ride over the high rail and the check rail simultaneously, increasing the necessary lateral force to cause a derailment. However, this ignores deficiencies in both track condition and check rail design. Deflection in the check rail between the supporting brackets will reduce much of the benefit. In addition, the dip caused by water run off at the end of the CD3P concrete pad causes the weight to lift off the leading wheels of the wagon, further reducing check rail effectiveness. In this case the moving of the check rail will not likely reduce the occurrences of derailments but may actually increase the severity.

The table below shows the results if the check rail is assumed to be polished by the passing of rail traffic.

| RAIL AND CHECK RAIL @60mm Gap | | | | | |
|---|---|---|---|---|---|
| RAIL SIDE L/V RATIO | | CHECK RAIL SIDE LV RATIO | | TOTAL L/V RATIO | % IMPROVEMENT |
| μ | L/V | μ | L/V | | |
| 0.5 | 0.26673269 | 0.5 | 1.088824063 | 1.355556752 | 33.51% |
| 0.5 | 0.26673269 | 0.6 | 0.933698423 | 1.200431113 | 18.23% |
| 0.5 | 0.26673269 | 0.7 | 0.810014662 | 1.076747352 | 6.05% |
| 0.5 | 0.26673269 | 0.8 | 0.709093134 | 0.975825824 | 0% |

Finally, it is worth taking note at how much the L/V ratio contributed by the rail side changes as the check rail is moved. The change in check rail placement has a minimal change in the check rail L/V ratio due to the contact point moving further out as the angle of attack decreases.

| Check Rail to Gauge Face Gap [mm] | Contact Angle [degrees] | Resulting Rail Side L/V Ratio (for μ=0.5) | Check Rail L/V ratio |
|---|---|---|---|
| 70 | 22.3 | -0.074576985 | 1.088824063 |
| 60 | 41.5 | 0.26673269 | 1.088824063 |
| 55 | 64.1 | 0.76829656 | 1.088824063 |

## 4.9 Increasing the check rail height

Moving the contact point onto the flat at the back of the wheel would create a huge difference in the Nadal ratio. The obvious way to do this is to raise the check rail height. It is not possible to go above the height of the fixing however the fixing is more than 12mm above the height of the check rail. The Nadal ratio for an angle of 90 degrees is as follows:

$$\left(\frac{L}{V}\right) = \frac{\tan(\theta) - \mu}{1 + \mu \times \tan(\theta)} = \frac{\tan(90) - 0.8}{1 + 0.8 \times \tan(90)} = 1.25$$

$$L = 1.444 \times V = 1.444 \times 2625 = 3790.5$$

If the coefficient of friction is taken at 0.5 the L/V ratio increases to 2. At first glance this is a large win however this effect is not actually realised. On closer inspection, as the check rail height is increased, the contact point moves up and out on the wheel. This leads to it still contacting on the curved surface on the outside of the wheel which creates the same 72-degree angle. It does however slightly increase the amount of time the lateral force must be applied to create a derailment.

## 4.10 Summary

It is clear that abrupt changes in the vertical direction in either OR both the high leg OR the low leg significantly increases the risk of wheel climb derailments. This situation is further exacerbated by the abrupt shift from tangent to relatively tight curve, with bogies that have much less steering ability when the wagons are empty.

The role of vertical dips in the running surface combined with high indexing forces is further indicated by the fact that the derailments at both dumpers took place at the same physical location, i.e. the drop- off from the concrete apron to the sleepered track, despite the fact that high longitudinal forces are present in the wagons both ahead and behind this position.

In addition to the supporting information it is shown historically that, derailments at CD3P ceased for a period of 18 months after the re-rail of the high leg, at which time the sleepered section was reportedly also realigned.

Monitoring of the vertical alignment should be introduced as a routine task, but need not be costly or time consuming. While detailed track measurements would be desirable, it should be noted that low angle photos at the right position such as those presented in this report can provide a permanent record of any significant dips that may be present, and can be made from positions of safety, rather than taking possession of this location or suspending normal dumper operations. While periodic realignment with a tamper is considered an effective containment measure, long term rectification would require dramatic improvement of the drainage at this position.

Given the burden of fines, causing ballast contamination in this area, any drainage option would obviously need to be designed to avoid clogging.

The Nadal calculation from the proposed alteration shows an ideal improvement of 77% lateral force resistance over the current case.

If the track is kept in good condition, the check rail can be moved closer to increase its effectiveness.

# Chapter 5 Chapter 5 – CONCLUSIONS

## 5.1 Project outcomes

Evaluation of the above information and consideration of the mechanisms involved in the flange climb derailments indicates that the installation of a fit for purpose check rail would provide some benefit, however the ability to reduce the occurrences by maintaining rail profile and reducing in train forces by reducing the indexing arm forces is likely to provide a more cost effective outcome.

## 5.2 Further work to be done

The closure of the gap at the check rail may work in the short term measure, but this is an unproven approach, and may introduce new issues that are not anticipated.
The inclusion of the check rail may see any vertical dips may be allowed to progress to comparable or worse levels rather than being resolved.
Further work needs to be completed to ensure the yard limits for rail wear is considered for specific locations and the rail network maintenance team implement the recommendations.

## 5.3 Recommendations

From the above considerations it is concluded that there are four distinct containment measures to significantly reduce the risk of derailments:

1. Further reductions in the dumper torque when dumping the last quarter of the tag, to limit the peak compressive forces on the empty wagons; and/or
2. Effective monitoring and intervention of any vertical misalignment at the concrete apron to sleepered track sections and reduction in checkrail gap.
3. Re-rail the high leg curve on a more regular basis and when the side wear of the rail has reached 50% of the mainline limit.
4. Remove the dip and eliminate re-occurrence by fixing drainage at both CD3P and CD4P and replacing ballast, gluing the ballast to ensure adequate transition stiffness.

# List of References


1. RailTrack PLC, Rolling Contact Fatigue in Rails; A Guide to Current Understanding and Practice, RT/PWG/0001, Issue 1, RailTrack PLC, UK; February 2001.

2. Epp, K., D. Welsby, Rail Profile Monitoring Report #3 for Rio Tinto – Pilbara Iron Rail Division, Report No. Monash/RT/2009/386, Monash University IRT, Melbourne Australia; February 2009.

3. International Heavy Haul Association (IHHA), Guidelines to Best Practices for Heavy Haul Railway Operations: Wheel and Rail Interface Issues, IHHA, Virginia Beach VA U.S.A.; May 2001.

4. Huimin Wu and Nicholas Wilson 2006, 'Railway vehicle Derailment and Prevention', in Simon Inwnicki (ed), Handbook of Railway Vehicle Dynamics, Taylor and Francis Group London.

5. Jean-Bernard Ayasse and Hugues Chollet 2006, 'Wheel – Rail Contact', in Simon Inwnicki (ed), Handbook of Railway Vehicle Dynamics, Taylor and Francis Group London.

6. Shu, X. and N. Wilson. TCRP Research Results Digest 82: Use of Guard/Girder/Restraining Rails. Transportation Research Board, The National Academies, Washington, D.C., 2007.

7. Wu, H., X. Shu, N. Wilson, and W. Shust. TCRP Report 71, Track- Related Research, Volume 5: Flange Climb Derailment Criteria and Wheel/Rail Profile Management and Maintenance Guidelines for Transit Operations. Transportation Research Board, National Research Council, Washington, D.C., 2005.

8. Griffin, T. Interfleet Technology, Inc., TCRP Report 114: Center Truck Performance on Low-Floor Light Rail Vehicles. Transportation Research Board, National Research Council, Washington, D.C., 2006.

9. Elkins, J., J. Peters, G. Arnold, and B. Rajkumar. "Steady-state Curving and Wheel/Rail Wear Properties of a Transit Vehicle on the Tight Turn Loop." UMTA-CO-06-0009-83-1, Washington, D.C., Dec. 1982.

10. Shu, X. and J. Tunna. "Investigation into Flange Climbing Derail- ment and Distance Criterion with Wheel and Worn Rail Profiles." Research Report R-982, Association of American Railroads, Trans- portation Technology Center, Inc.,

Feb. 2007.

11. RISSB (Rail Industry Safety and Standards Board) 2013, Derailment Investigation and Analysis Guideline.

12. Roger Lewsi and Rob Dwyer-Joyce 2006, ‘Industrial Lubrication Practice – Wheel/Rail Tribology’, in Simon Inwnicki (ed), Handbook of Railway Vehicle Dynamics, Taylor and Francis Group London.

13. Tournay, H. 2001, Supporting technologies vehicle track interaction, in *Guidelines to best Practice for Heavy Haul Railway Operations: Wheel and Rail Interface Issues*, International Heavy Haul Association, Virginia Beach USA, 2-1-2.73.

# Appendix A - Project Specification

University of Southern Queensland

FACULTY OF ENGINEERING AND SURVEYING

**ENG4111/4112 Engineering Research Project**
PROJECT SPECIFICATION

AUTHOR: Lindsay Dobson

TOPIC: **DUMPER DERAILMENT INVESTIGATION AND DEVELOPMENT OF CUSTOM CHECK RAIL**

SUPERVISOR: STEVEN GOH

ENROLMENT ENG4111 – EXT S1, 2016
ENG4112 – EXT S2, 2016

PROJECT AIM: To investigate the underlying causes and site specific conditions contributing to the regular derailments at CD3 and CD4.
Develop a rectification methodology, including the development of a replacement fit for purpose checkrail.
Identify and deliver maintenance recommendations for the new checkrail

**PROGRAMME: (VERSION1, 14/03/2016)**

1. Research previous failures on network relating to track geometry and check rail position
2. Conduct site investigation and measurement of existing track geometry
3. Review incident reports from historical derailments
4. Review of historical "as constructed" drawings
5. Conduct assessment of wheel position
6. Assessment of existing checkrail effectiveness
7. Design of new customised checkrail
8. Complete cost evaluation of proposed design installation
9. Develop maintenance plan and methodology

*If time permits produce scope of work to install checkrail to CD3 and CD4

# Appendix B - Historical Derailments

| Date | Location | Position | Car Number | Tag | Assumed Cause | Incident Number |
|---|---|---|---|---|---|---|
| 29/6/2016 | CD4P | 225 | B25045 | 45 | Track Design/Maintenance | 1000438148 |
| 28/6/2016 | CD4P | 217 | B25270 | 44 | Track Design/Maintenance | 1000437301 |
| 12/03/2016 | CD4P | 221 | B25019 | 47 | Track Design/Maintenance | |
| 5/03/2016 | CD4P | 217 | HI7210 | 24 | Track Design/Maintenance | 1000428150 |
| 20/02/2016 | CD3P | 223 | C15759 | 15 | Track Design/Maintenance | 1000426863/ 1000426866 |
| 17/01/2016 | CD3P | 209 | B25040 | 37 | Track Design/Maintenance | 1000423810 |
| 6/07/2015 | CD3P | 225 | B25186 | 46 | Track Design/Maintenance | 1000332788 |
| 4/03/2015 | CD4P | 226 | B25470 | 37 | Track design/Maintenance | 1000328593 |
| 3/04/2015 | CD3P | | | | | 1000325266 |
| 21/07/2014 | CD3P | 217 and 223 | HI8390 and HI8395 | | Track design/Maintenance | 1000286258 |
| 28/05/2014 | CD3P | 232 | HI7504 | | driver notched up too fast | |
| 21/04/2014 | CD4P | | N/A | | CD4P fault/error -> check | |
| 9/12/2013 | CD3P | 175 | HI7280 | | Track Design/Maintenance | 1000255885 |
| 1/05/2012 | CD4P | N/A | | | New Q series slipped out of dumper | |
| 6/03/2012 | CD3P | not available | | | Track Design/Maintenance | |
| 30/11/2012 | CD4P | not available | | | CD4P tail track 280 points | 1000175261 |
| 3/06/2012 | CD3P | 206 | 8747 | 34 | 6 cars from CD3P | 1000136376 |
| 17/02/2012 | CD3P | not available | 6887 | | Track design/maintenance | 1000117510 |
| 12/06/2010 | CD3P | not available | 6613/1599 | | CD3P derailed no detail | 1000071538 |
| 18/03/2010 | CD4P | not available | | | derailment of empty ore cars no detail | 1000065144 |

# Appendix C - Risk Assessment

Rio Tinto

## HSEQ Qualitative Risk Analysis (Level 2) - Workshop Record Sheet

To record Predicted Risk unhide columns AF-AH

| RISK HEADER | | | | RISK SCENARIO | | | INHERENT RISK - Optional Data Capture | | | | CURRENT RISK - mandatory data capture | | | | | | | | IMPROVEMENT ACTIONS - proposed new controls | | |
|---|---|---|---|---|---|---|---|---|---|---|---|---|---|---|---|---|---|---|---|---|---|
| Mandatory Rio Tinto Defined | Mandatory Rio Tinto Defined | Mandatory Rio Tinto Defined | Mandatory Rio Tinto Defined | Mandatory Free Text | Mandatory Rio Tinto Defined | Mandatory Rio Tinto Defined | Optional Rio Tinto Defined | Optional Rio Tinto Defined | Optional Rio Tinto Defined | Optional Free Text | Optional Rio Tinto Defined | Mandatory Rio Tinto Defined | Mandatory Free Text | Optional Free Text | Mandatory Rio Tinto Defined | Mandatory Rio Tinto Defined | Mandatory Rio Tinto Defined | Optional Free Text | Optional Free Text | Optional Business Defined | Optional Free Text |
| Risk ID | Hazard Type | Hazard Description (Sub-Type) | Operational Status | Scenario Description | Consequence Category | Consequence Sub-Category | Consequence | Likelihood | Risk Rating | Risk Comments | Cause Description | Control Type Description | Control Comments | Impact Description | Consequence | Likelihood | Risk Rating | Risk Comments | Action Description | Action Owner Position | Action Status / Comments |
| P01 | Mechanical | Mass and Stability | Normal Operation | **EXISTING MAINTAINED RISK PROFILE**<br>Existing track section in specification with correct geometry, alignment and existing check rail in place. Wagons derail and cause dumper shut and inability to offload wagons | Production volumes | Quantity / output | 2-Medium | D-Unlikely | Low | Risk consequence and likelyhood taken from information pre installation of existing checkrail. | Equipment difficulty | 4 Administrative Controls | **Existing track system:**<br>Regular maintenance<br>Correct alignment<br>Within geometry specification.<br>Limited gauge face wear<br>Ballast bonding | Existing section was derailment free for 18 months following the completion of a rerail and realignment. | 2-Medium | D-Unlikely | Low | Risk rating consequence has been assumed to impact train losses for 1 day on both outgoing lines | | | |
| P02 | Mechanical | Mass and Stability | Normal Operation | **CURRENT RISK PROFILE**<br>Existing track section allowed to develop geometry misalignment before crossing, causing intrain forces and wheel flange climb to derail wagons resulting in dual line dumper closure. | Production volumes | Quantity / output | 2-Medium | B-Likely | High | Inherent risk does not consider inclusion of checkrail. Risk consequence and likelyhood taken from information pre installation of existing checkrail and rerail of section in 2010. Information presented for the CEA justification of the checkrail installation estimated the lost tonnes of 450,000T p.a. | | 3 Engineering Controls | **Install checkrail with existing 100mm gap**<br>Is currently installed and proving to provide minor control and risk reduction | Checkrail does not adequately control derailment likelyhood due to flange climb and flange position on high leg of curve. See report '*CD3P and CD4P Check Rail Modification*' date:13 August 2014<br>Likelyhood of derailment does not significantly decrease. | 2-Medium | B-Likely | High | | | | |
| P03 | | | | | | | | | | | | 3 Engineering Controls | **Install checkrail with proposed 60mm gap Mild Steel** | Checkrail may not adequately control derailment likelyhood due to flange climb and flange position on high leg of curve. New installation has possibility of loco wheelset binding, excessive high leg gauge face wear, therefore increasing track gauge resulting in excessive checkrail wear.<br>Likelyhood of derailment does not significantly decrease. Calcualtions using Nadal equation suggest improvement in the order of 20% | 2-Medium | B-Likely | High | Interem solution of closing the gap may not realise the risk reduction initally estimated. An improvement of 20% does not necessarily translate to a reduction in the likelihood of derailment. | | | |
| P04 | | | | | | | | | | | | 3 Engineering Controls | **Install custom designed active checkrail**<br>*Checkrail designed to suit location and variability in wheel configuration<br>*L/V ratio optimised for location | Custom checkrail adequately spaced and optimised for the location could offer theoretical improvement of 100% based on a doubling of weight in the Nadal equation.<br>Failure to remove track dip reduces effectiveness. Solution assumes hostorical track maintenance and possible return of dip. | 2-Medium | C-Possible | Moderate | Installation of custom checkrail will reduce likelihood. Inclusion of DED's should be considered as part of the overall solution to reduce the impact and therefore maximum reasonable consequence of flange climb derailment. | | | |
| P05 | | | | | | | | | | | | 3 Engineering Controls | **Install custom active checkrail and transition track stiffness of the section to end of concrete slab.** | Installation of custom checkrail and transition section will provide a system to ensure better track geometry and also provide an additional control for flange climb. Likelyhood is evidenced by 18 month gap in derailments from 2010 when the section was realigned and re-railed. Transition section assumes the dip will be eliminated. | 2-Medium | D-Unlikely | Low | | | | |
| P06 | Mechanical | Mass and Stability | Normal Operation | **INSTALLATION OF A CHECKRAIL WITH 60mm GAP**<br>**Installation causes any of the listed issues, resulting in derailment and dumper closure**<br>- Locomotives long wheel base to have excessive rolling resistance against the check rail.<br>- A single wheel is captured between the check rail and low leg can cause wheel chatter and wheel climb<br>- Wheels bite into mild steel check rail assisting a flange climb<br>- Wear rate of mild steel reduces check rail effectiveness<br>- Bracket spacing is 2365mm which could potentially allow the check rail to deflect allowing the wheels to ride over it<br>- Narrow back to back and worn rail/wheel causing the check rail to be constantly contacted. | Production volumes | Quantity / output | 2-Medium | B-Likely | High | **Inherant risk is taken from line P03. Individually each hazard likelihood will rate lower than the overall liklihood. Likelihood of at least 1 event occuring increases the overall occurrence likelihood and will increase the risk rating.** | Equipment difficulty-Design | 3 Engineering Controls | **Peer check engineering design**<br>Check gap width by calculation and simulation to ensure gap is wide enough. Calculation to allow for center axle floats. Installation to ensure geometry check and post installation observation. | Locomotive Derailment, check rail damage | 1-Minor | C-Possible | Low | Locomotive derailment may not cause closure of dumper line, however is assumed to cause damage to the rail and therfore envoke a minor consequence, due to shorter down time and lower value losses. | | | |
| P07 | | | | | | | | | | | | 4 Administrative Controls | **Post installation monitoring and preventative maintenance**<br>On site checks and maintenance to ensure checkrail remains within tolerances | Derailment, check rail damage | 2-Medium | D-Unlikely | Low | Maintenance tactics have historically been unable to maintain required parameters for existing configuration. Due to the nature of the issue, adequate maintenance is seen as the largest contributiong factor to derailment reduction. | **Whilst Each of these individual controls may reduce the likelihood when considered in isolation, the probability that at least one of these will happen is still Likely and the consequence is the same as the inherent risk being medium. With this considered the risk reduction by installing a temporary solution at this location and reducing the gap to 60mm will not be realised.** | | |
| P08 | | | | | | | | | | | | 3 Engineering Controls | **Alter Checkrail profile**<br>Chamfer mild steel billets in attempt to reduce likelihood of flange climb | Derailment, check rail damage | 2-Medium | C-Possible | Moderate | Champher of edge on mid steel rail will not be as effective as custom checkrail and will not guarantee reudction in climb | | | |
| P09 | | | | | | | | | | | | | | | | | | | | | |
| P10 | | | | | | | | | | | | 3 Engineering Controls | **Increase checkrail stiffness by adding brackets**<br>Billet makes it stiffer, wheel must already have started riding up the high leg. Geometry checks so it is not always contacting hard against the check rail | Derailment, check rail damage | 1-Minor | C-Possible | Low | Likely to occur with Locomotive impact due to weight and deflection, therefore reducing the consequence impact. | | | |
| P11 | | | | | | | | | | | | 3 Engineering Controls | **Ensure design adequately considers worn wheel/Rail impact**<br>geometry check with worn rail, wheels and tightest back to back | Derailment, check rail damage | 2-Medium | C-Possible | Moderate | Due to variability in tolerances with wheel and rail wear, caluculation of optimal gap with temporary checkrail design will still see the liklihood as possible. | | | |
| P12 | Social / Cultural | Stakeholder Expectations | | Rail Engineering suffers reputational damage due to solutions failing to appreciably change derailment frequency. | Rio Tinto or Business Unit Reputation | Negative | 1-Minor | B-Likely | Moderate | In the current situation without changes to the underlying issues including maintenance tactics and induced in train forces, the likelyhood of derailment is not significantly reduced. | Management system | 4 Administrative Controls | **Do not install temporary solution**<br>Historical work combined with engineering design, likely outcome assessment and risk impact assessment indicate that the only feasible checkrail solution should be a custom designed solution. The installation of a temporary measure is likely to be seen as a failure by stakeholders. Higher initial cost is the main impact of choosing a custom solution. | Loss of future opportunity to provide engineering support amonst stakeholders within RTIO. Possible negative ONSR implications. Loss of credibility and professional standing | 1-Minor | B-Likely | Moderate | Due to stakeholder expectation and understanding of checkrail, temporary makeshift repair may be seen as solution to derailment problem. If a subsequent derailment occurs, despite not being the optimal checkrail solution the stakeholdr expectation will n and cause reputational damage to the Dept | **Custom checkrail solution to be further investigated by Rail Engineering. Solution to investigate Cost V Benefit analysis in addition to business risk.<br>Risk Assessment of the solution will be captured as part derailment investigation already being undertaken.** | Principal – Mechanical & Network Infrastructure | |
| P13 | | | | | Compliance impact | License - external (potential) | 1-Minor | D-Unlikely | Low | It is unlikely that a compliance impact will be realised unless a number of hazards align and due process has not been followed. | Management system | 4 Administrative Controls | **Compliance with engineering design principals and change management process**<br>Maintaining existing standards and following approved process will ensure compliance. | Loss of license to operate amonst stakeholders within RTIO. Possible negative ONSR implications | 1-Minor | D-Unlikely | Low | It is unlikely that a compliance impact will be realised unless a number of hazards align and due process has not been followed. | | | |

L2RA - 50mm billet to front of check rail.xlsx
Version 1.0
Uncontrolled when printed
See document mangement system for current document

Page 1 of 1
Copyright Statement

Internal Use Only

# Appendix D - Rail Profile

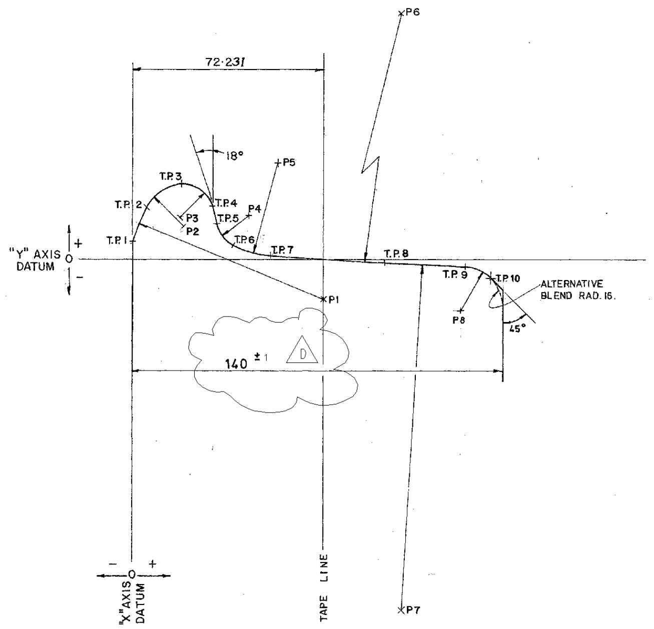


| RADIUS CENTRE CO-ORDINATES | | | | |
|---|---|---|---|---|
| | CENTRE № | 'X' AXIS | 'Y' AXIS | RADIUS |
| GROUP 1 (TOLERANCES) | P1 | +72·23 | -15·06 | 75·41 |
| | P2 | +19·39 | +12·36 | 15·88 |
| | P3 | +17·80 | +15·74 | 12·50 |
| | P4 | +43·60 | +16·54 | 12·40 |
| | P5 | +54·60 | +36·34 | 35·00 |
| GROUP 2 (TOLERANCES) | P6 | +125·10 | +898·44 | 900·00 |
| | P7 | +78·60 | -500·76 | 500·00 |
| | P8 | +123·81 | - 18·89 | 16·00 |

| TANGENT POINT CO-ORDINATES | | | | |
|---|---|---|---|---|
| | T. P. № | 'X' AXIS | 'Y' AXIS | — |
| GROUP 1 (TOLERANCES) | T.P.1 | 0·00 | + 6·61 | — |
| | T.P.2 | + 5·29 | +19·67 | — |
| | T.P.3 | +17·80 | +28·24 | — |
| | T.P.4 | +29·60 | +19·74 | — |
| | T.P.5 | +31·80 | +13·04 | — |
| | T.P.6 | +37·60 | + 5·74 | — |
| | T.P.7 | +51·70 | + 1·44 | — |
| | T.P.8 | +95·20 | - 1·06 | — |
| | T.P.9 | +125·30 | - 2·96 | — |
| | T.P.10 | +135·12 | - 7·58 | — |

**GENERAL TOLERANCES**

± 0·25 mm FOR GROUP 1

± 1·0% FOR GROUP 2

NOTE
THIS PROFILE MAY BE USED IN SPECIFICATIONS FOR NEW WHEELS
IT SHOULD NOT BE USED AS A PROFILE FOR WHEEL LATHE TEMPLATES.

| REV | BY | DATE | DESCRIPTION | CKD | APP |
|---|---|---|---|---|---|
| D | MSC | 9-11-99 | SCANNED & RV GENERATED TOL. REVISED WAS +/- 3 | | PRC |

| | | |
|---|---|---|
| DRAWN | RJM | 1-11-82 |
| TRACED | | |
| CHECKED | JGR | 1-11-82 |
| SUPT DRAFT | | |
| PROJ. ENG. | | |
| APPROVED | JGR | 1-11-82 |
| APPROVED FOR CONSTRUCTION | | |

TOTAL WEIGHT | ITEM | SUB ITEM | REQ'D | DESCRIPTION OR MATERIAL QUANTITY | REMARKS

HAMERSLEY IRON PTY. LIMITED — WESTERN AUSTRALIA ACN 004 558 276

RAILWAYS 7 MILE
ROLLINGSTOCK
NEW WHEEL TREAD PROFILE
DETAILS

SCALE 1:1
DRAWING No RM-008-049 REV D
PN No

SHEET SIZE A2 | REFERENCES | REVISIONS

# Appendix E - Checkrail Design

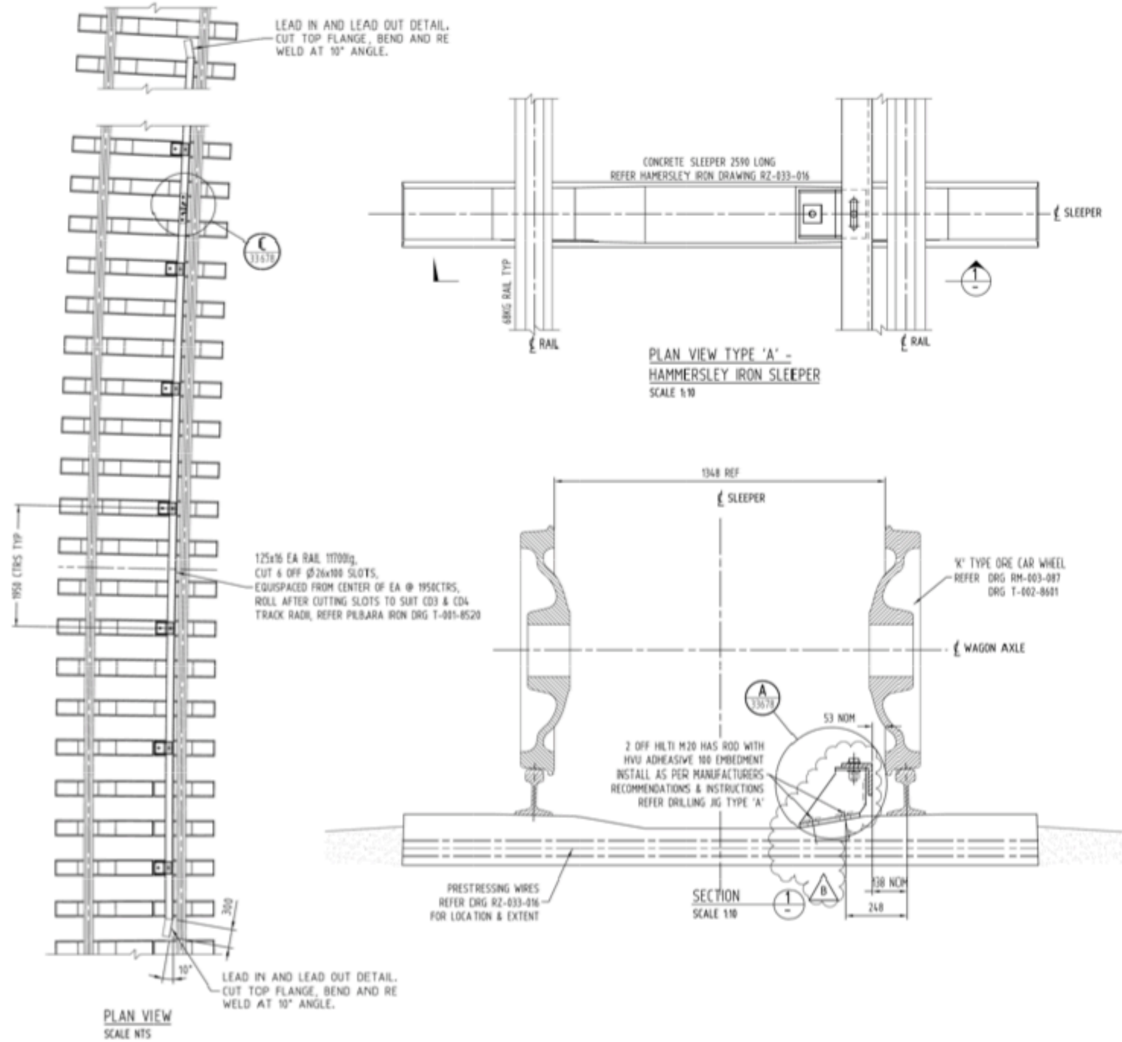

# Appendix F - Maintenance Track Geometry Limits

Within the current track configuration, it is Rio Tinto Iron Ore Railways Division requirement to:

- Attempt to achieve at least the value of those figures listed in Table 7 under "Target Level" for the respective parameters described and for the respective Classes of track.
- As soon as practicable, carry out corrections to the track where the measured value of a particular parameter exceeds a value of the order of those listed under "Tolerance Level" in Table 7 for the respective parameters described and for the respective Classes of track.
- Take immediate precautionary and corrective action to the track where the measured value of a particular parameter exceeds a value listed under "Critical Level" in Table 7 for the respective parameters described and for the respective Classes of track

The measurement of track geometry is intended to be carried out with a TRV for Class A tracks and for Class B & C track the measurements shall be made manually / by measuring trolley in accordance with the standards set out in Table 7.

**Table 7 – Track Geometry Limits**

| Parameter | Class of Track | Target (mm) | Defect (mm) | Critical (mm) |
|---|---|---|---|---|
| Twist<br>2m/8m chords | A<br>B<br>C | 3<br>4<br>6 | 8<br>14<br>16 | 12<br>18<br>18 |
| Top<br>5.983m chord | A<br>B<br>C | 5<br>7<br>10 | 7<br>14<br>16 | 12<br>20<br>20 |
| Top<br>10m chord | A<br>B<br>C | 9<br>12<br>18 | 12<br>24<br>28 | 21<br>35<br>35 |
| Line 7.925m | A<br>B<br>C | 4<br>6<br>12 | 10<br>20<br>23 | 16<br>26<br>26 |
| Line 10m: | A<br>B<br>C | 6<br>9<br>18 | 13<br>26<br>30 | 21<br>35<br>35 |
| Min Gauge: | A<br>B<br>C | 1433 (-2)<br>1433 (-2)<br>1430 (-5) | 1430 (-5)<br>1425 (-10)<br>1423 (-12) | 1428 (-7)<br>1421 (-14)<br>1421 (-14) |
| Max Gauge: | A<br>B<br>C | 1443 (+8)<br>1450 (+15)<br>1455 (+20) | 1445 (+10)<br>1455 (+20)<br>1457 (+22) | 1453 (+18)<br>1460 (+25)<br>1460 (+25) |

| | | | | |
|---|---|---|---|---|
| Crosslevel (Deviation from Applied Superelevation) | N/A | 5 | 10 | 20 |

## Twist Defect

The difference between the cross levels over a defined length (i.e. the difference in level of the two rails).
'Short' and 'long' twist are specified to ensure that rolling stock can negotiate a twist without wheel unloading.

- Short twist, measured over 2m or a similar length is representative of the axle spacing for freight and passenger bogies for most railway operations.
- 'Long' twist, measured over 8m or a similar length is representative of the minimum rolling stock length for most railway operations. Ore cars used by Rio Tinto are significantly shorter than most other bogie rolling stock, including other heavy haul railways, and therefore a long twist length of 8m is used on the Rio Tinto Network.

The high load to tare ratio of the ore cars also impacts on the ability of the designers to optimise the suspension characteristics to cope with track twist.

# Appendix G - Derailment Information

| Wheel Profile | mm | AAR |
|---|---|---|
| 8 | | |
| Flange Thickness (mm) | 32.30 | 0 |
| Flange Height (mm) | 27.10 | |
| Rim Thickness (mm) | 63.50 | 40 |
| Tread Hollow (mm) | 0.00 | |
| Brake Shoe (mm) | 5.09 | |

| Wheel Profile | mm | AAR |
|---|---|---|
| 7 | | |
| Flange Thickness (mm) | 32.50 | 0 |
| Flange Height (mm) | 27.10 | |
| Rim Thickness (mm) | 59.40 | 37 |
| Tread Hollow (mm) | 0.00 | |
| Brake Shoe (mm) | 9.30 | |

| Wheel Profile | mm | AAR |
|---|---|---|
| 6 | | |
| Flange Thickness (mm) | 33.20 | 0 |
| Flange Height (mm) | 27.00 | |
| Rim Thickness (mm) | 60.90 | 38 |
| Tread Hollow (mm) | 0.00 | |
| Brake Shoe (mm) | 3.41 | |

| Wheel Profile | mm | AAR |
|---|---|---|
| 5 | | |
| Flange Thickness (mm) | 31.40 | 1 |
| Flange Height (mm) | 27.10 | |
| Rim Thickness (mm) | 61.40 | 39 |
| Tread Hollow (mm) | 0.00 | |
| Brake Shoe (mm) | 20.47 | |

| Wheel Profile | mm | AAR |
|---|---|---|
| 4 | | |
| Flange Thickness (mm) | 33.10 | 0 |
| Flange Height (mm) | 27.00 | |
| Rim Thickness (mm) | 62.70 | 39 |
| Tread Hollow (mm) | 0.00 | |
| Brake Shoe (mm) | 32.82 | |

| Wheel Profile | mm | AAR |
|---|---|---|
| 3 | | |
| Flange Thickness (mm) | 33.10 | 0 |
| Flange Height (mm) | 27.00 | |
| Rim Thickness (mm) | 62.30 | 39 |
| Tread Hollow (mm) | 0.00 | |
| Brake Shoe (mm) | 17.23 | |

| Wheel Profile | mm | AAR |
|---|---|---|
| 2 | | |
| Flange Thickness (mm) | 33.00 | 0 |
| Flange Height (mm) | 26.90 | |
| Rim Thickness (mm) | 62.60 | 39 |
| Tread Hollow (mm) | 0.00 | |
| Brake Shoe (mm) | 8.33 | |

| Wheel Profile | mm | AAR |
|---|---|---|
| 1 | | |
| Flange Thickness (mm) | 32.70 | 0 |
| Flange Height (mm) | 26.90 | |
| Rim Thickness (mm) | 61.20 | 39 |
| Tread Hollow (mm) | 0.00 | |
| Brake Shoe (mm) | 10.93 | |

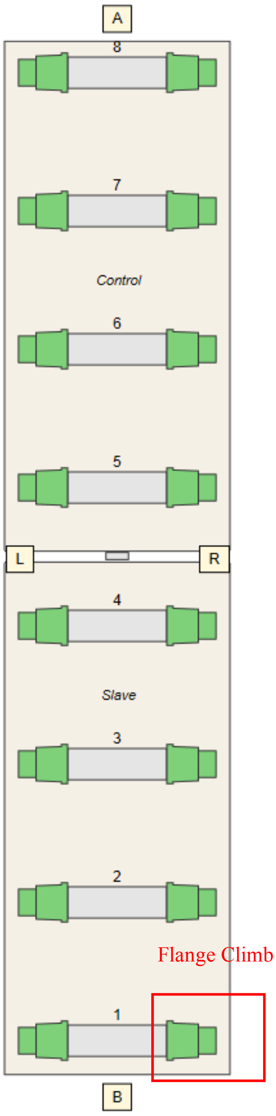


| Wheel Profile | mm | AAR |
|---|---|---|
| 8 | | |
| Flange Thickness (mm) | 31.90 | 0 |
| Flange Height (mm) | 26.60 | |
| Rim Thickness (mm) | 63.00 | 40 |
| Tread Hollow (mm) | 0.00 | |
| Brake Shoe (mm) | 34.37 | |

| Wheel Profile | mm | AAR |
|---|---|---|
| 7 | | |
| Flange Thickness (mm) | 33.10 | 0 |
| Flange Height (mm) | 26.50 | |
| Rim Thickness (mm) | 58.90 | 37 |
| Tread Hollow (mm) | 0.00 | |
| Brake Shoe (mm) | 16.10 | |

| Wheel Profile | mm | AAR |
|---|---|---|
| 6 | | |
| Flange Thickness (mm) | 32.21 | 0 |
| Flange Height (mm) | 26.30 | |
| Rim Thickness (mm) | 59.42 | 37 |
| Tread Hollow (mm) | -1.53 | |
| Brake Shoe (mm) | 12.71 | |

| Wheel Profile | mm | AAR |
|---|---|---|
| 5 | | |
| Flange Thickness (mm) | 33.00 | 0 |
| Flange Height (mm) | 26.60 | |
| Rim Thickness (mm) | 60.80 | 38 |
| Tread Hollow (mm) | 0.00 | |
| Brake Shoe (mm) | 7.61 | |

| Wheel Profile | mm | AAR |
|---|---|---|
| 4 | | |
| Flange Thickness (mm) | 33.70 | 0 |
| Flange Height (mm) | 26.40 | |
| Rim Thickness (mm) | 62.50 | 39 |
| Tread Hollow (mm) | 0.00 | |
| Brake Shoe (mm) | 30.82 | |

| Wheel Profile | mm | AAR |
|---|---|---|
| 3 | | |
| Flange Thickness (mm) | 33.70 | 0 |
| Flange Height (mm) | 26.50 | |
| Rim Thickness (mm) | 61.50 | 39 |
| Tread Hollow (mm) | 0.00 | |
| Brake Shoe (mm) | 19.23 | |

| Wheel Profile | mm | AAR |
|---|---|---|
| 2 | | |
| Flange Thickness (mm) | 32.90 | 0 |
| Flange Height (mm) | 26.60 | |
| Rim Thickness (mm) | 62.70 | 39 |
| Tread Hollow (mm) | 0.00 | |
| Brake Shoe (mm) | 10.56 | |

| Wheel Profile | mm | AAR |
|---|---|---|
| 1 | | |
| Flange Thickness (mm) | 32.40 | 0 |
| Flange Height (mm) | 26.60 | |
| Rim Thickness (mm) | 61.00 | 38 |
| Tread Hollow (mm) | 0.00 | |
| Brake Shoe (mm) | 18.80 | |

*1.1.1.1.1 FleetOne information for B20270*

## A.1 Vehicle Mimic B20045

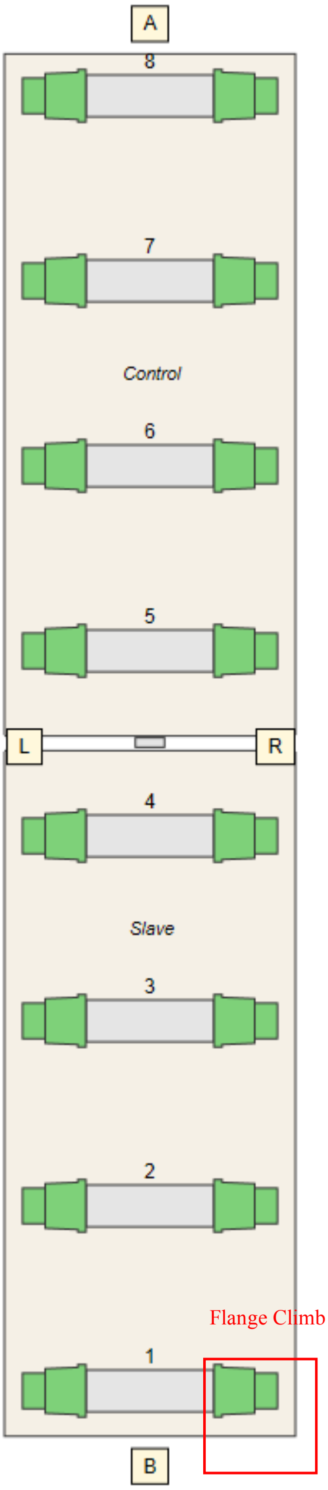


8

| Wheel Profile | mm | AAR |
|---|---|---|
| Flange Thickness (mm) | 31.50 | 1 |
| Flange Height (mm) | 26.64 | |
| Rim Thickness (mm) | 61.90 | 39 |
| Tread Hollow (mm) | -1.75 | |
| Brake Shoe (mm) | 27.09 | |

8

| Wheel Profile | mm | AAR |
|---|---|---|
| Flange Thickness (mm) | 31.33 | 1 |
| Flange Height (mm) | 26.36 | |
| Rim Thickness (mm) | 61.59 | 39 |
| Tread Hollow (mm) | -1.64 | |
| Brake Shoe (mm) | 30.62 | |

7

| Wheel Profile | mm | AAR |
|---|---|---|
| Flange Thickness (mm) | 31.79 | 0 |
| Flange Height (mm) | 26.42 | |
| Rim Thickness (mm) | 60.32 | 38 |
| Tread Hollow (mm) | -1.88 | |
| Brake Shoe (mm) | 31.94 | |

7

| Wheel Profile | mm | AAR |
|---|---|---|
| Flange Thickness (mm) | 31.83 | 0 |
| Flange Height (mm) | 26.42 | |
| Rim Thickness (mm) | 60.44 | 38 |
| Tread Hollow (mm) | -1.44 | |
| Brake Shoe (mm) | 26.61 | |

6

| Wheel Profile | mm | AAR |
|---|---|---|
| Flange Thickness (mm) | 32.30 | 0 |
| Flange Height (mm) | 26.56 | |
| Rim Thickness (mm) | 59.80 | 38 |
| Tread Hollow (mm) | -1.68 | |
| Brake Shoe (mm) | 8.55 | |

6

| Wheel Profile | mm | AAR |
|---|---|---|
| Flange Thickness (mm) | 31.58 | 1 |
| Flange Height (mm) | 26.44 | |
| Rim Thickness (mm) | 59.89 | 38 |
| Tread Hollow (mm) | -1.53 | |
| Brake Shoe (mm) | 20.53 | |

5

| Wheel Profile | mm | AAR |
|---|---|---|
| Flange Thickness (mm) | 30.97 | 1 |
| Flange Height (mm) | 26.61 | |
| Rim Thickness (mm) | 61.31 | 39 |
| Tread Hollow (mm) | -1.79 | |
| Brake Shoe (mm) | 32.11 | |

5

| Wheel Profile | mm | AAR |
|---|---|---|
| Flange Thickness (mm) | 31.30 | 1 |
| Flange Height (mm) | 26.59 | |
| Rim Thickness (mm) | 61.56 | 39 |
| Tread Hollow (mm) | -1.46 | |
| Brake Shoe (mm) | 8.19 | |

4

| Wheel Profile | mm | AAR |
|---|---|---|
| Flange Thickness (mm) | 31.44 | 1 |
| Flange Height (mm) | 26.54 | |
| Rim Thickness (mm) | 61.68 | 39 |
| Tread Hollow (mm) | -1.78 | |
| Brake Shoe (mm) | 25.48 | |

4

| Wheel Profile | mm | AAR |
|---|---|---|
| Flange Thickness (mm) | 31.71 | 0 |
| Flange Height (mm) | 26.18 | |
| Rim Thickness (mm) | 61.89 | 39 |
| Tread Hollow (mm) | -1.61 | |
| Brake Shoe (mm) | 24.81 | |

3

| Wheel Profile | mm | AAR |
|---|---|---|
| Flange Thickness (mm) | 32.42 | 0 |
| Flange Height (mm) | 26.57 | |
| Rim Thickness (mm) | 61.33 | 39 |
| Tread Hollow (mm) | -1.83 | |
| Brake Shoe (mm) | 9.30 | |

3

| Wheel Profile | mm | AAR |
|---|---|---|
| Flange Thickness (mm) | 31.75 | 0 |
| Flange Height (mm) | 26.45 | |
| Rim Thickness (mm) | 61.28 | 39 |
| Tread Hollow (mm) | -1.42 | |
| Brake Shoe (mm) | 9.67 | |

2

| Wheel Profile | mm | AAR |
|---|---|---|
| Flange Thickness (mm) | 32.05 | 0 |
| Flange Height (mm) | 26.53 | |
| Rim Thickness (mm) | 61.80 | 39 |
| Tread Hollow (mm) | -1.66 | |
| Brake Shoe (mm) | 9.47 | |

2

| Wheel Profile | mm | AAR |
|---|---|---|
| Flange Thickness (mm) | 31.75 | 0 |
| Flange Height (mm) | 26.50 | |
| Rim Thickness (mm) | 62.29 | 39 |
| Tread Hollow (mm) | -1.60 | |
| Brake Shoe (mm) | 32.35 | |

1

| Wheel Profile | mm | AAR |
|---|---|---|
| Flange Thickness (mm) | 31.14 | 1 |
| Flange Height (mm) | 26.47 | |
| Rim Thickness (mm) | 63.19 | 40 |
| Tread Hollow (mm) | -1.89 | |
| Brake Shoe (mm) | 29.88 | |

1

| Wheel Profile | mm | AAR |
|---|---|---|
| Flange Thickness (mm) | 30.99 | 1 |
| Flange Height (mm) | 26.42 | |
| Rim Thickness (mm) | 63.21 | 40 |
| Tread Hollow (mm) | -1.63 | |
| Brake Shoe (mm) | 7.53 | |

*1.1.1.1.2 FleetOne information for B20045*

## A.2 WID System

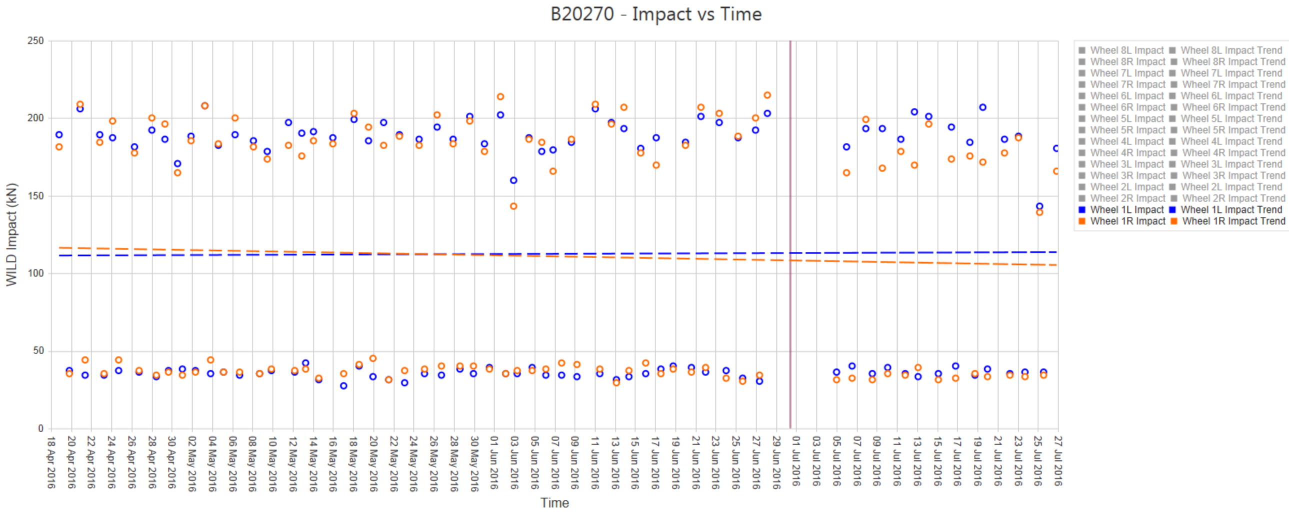


*1.1.1.1.3 B20270 derailed wheel set WID impact trend*

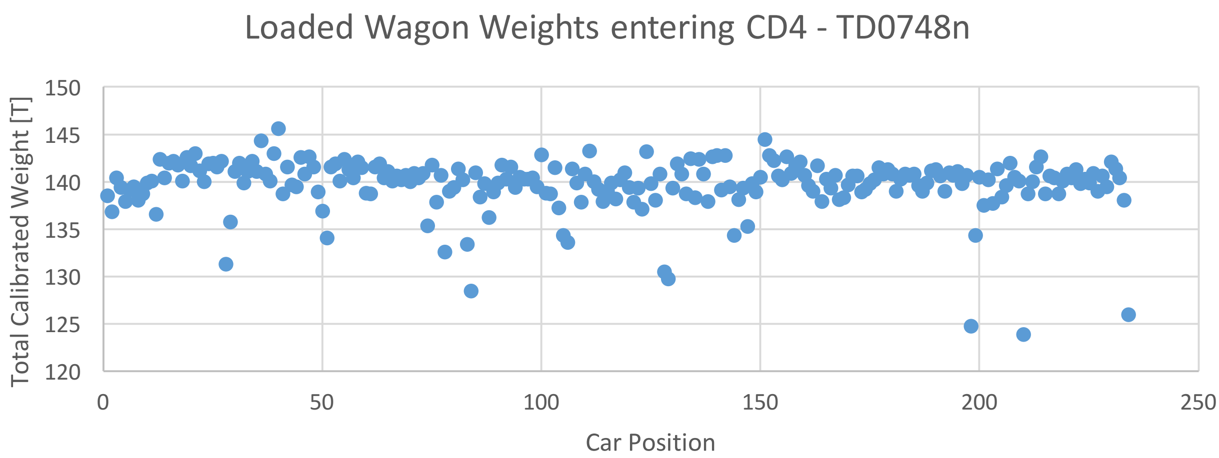


*1.1.1.1.4 B20270 WID wagon weights*

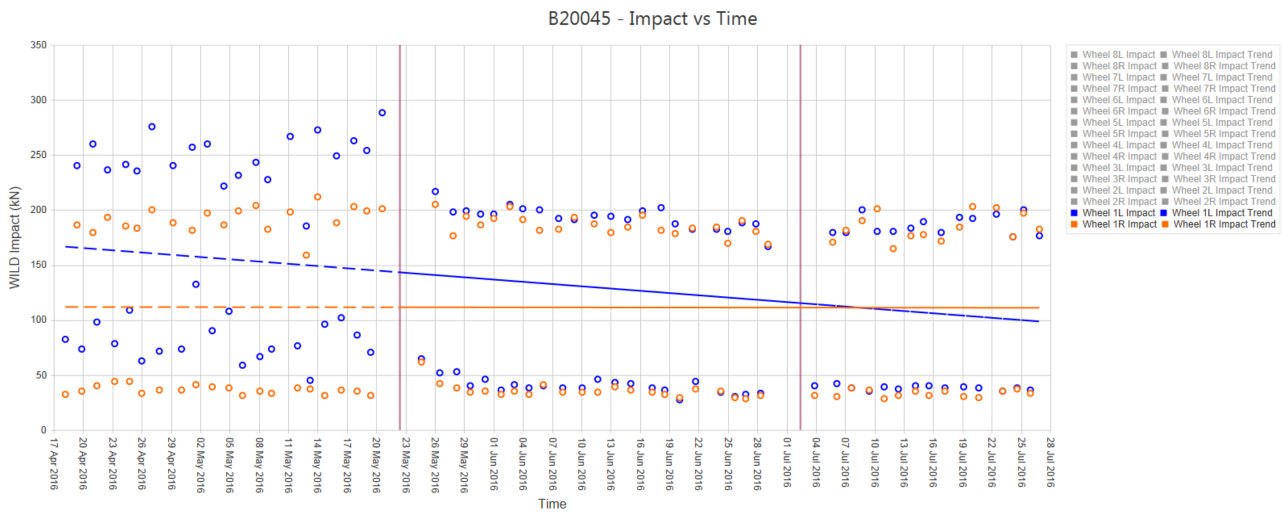


*1.1.1.1.5 B20045 derailed wheel set WID impact trend*

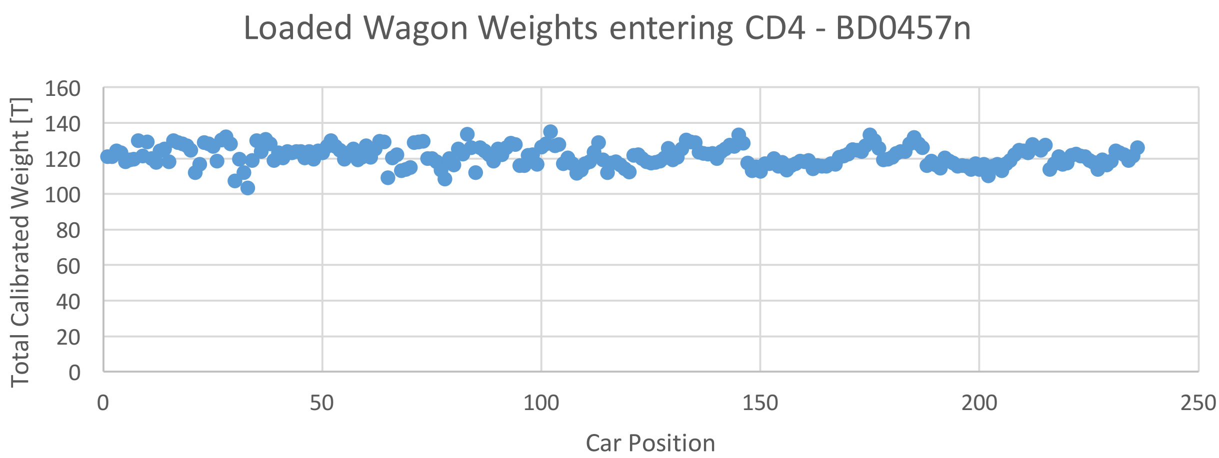


*1.1.1.1.6 B20045 WID wagon weights*

## A.3 HBD System

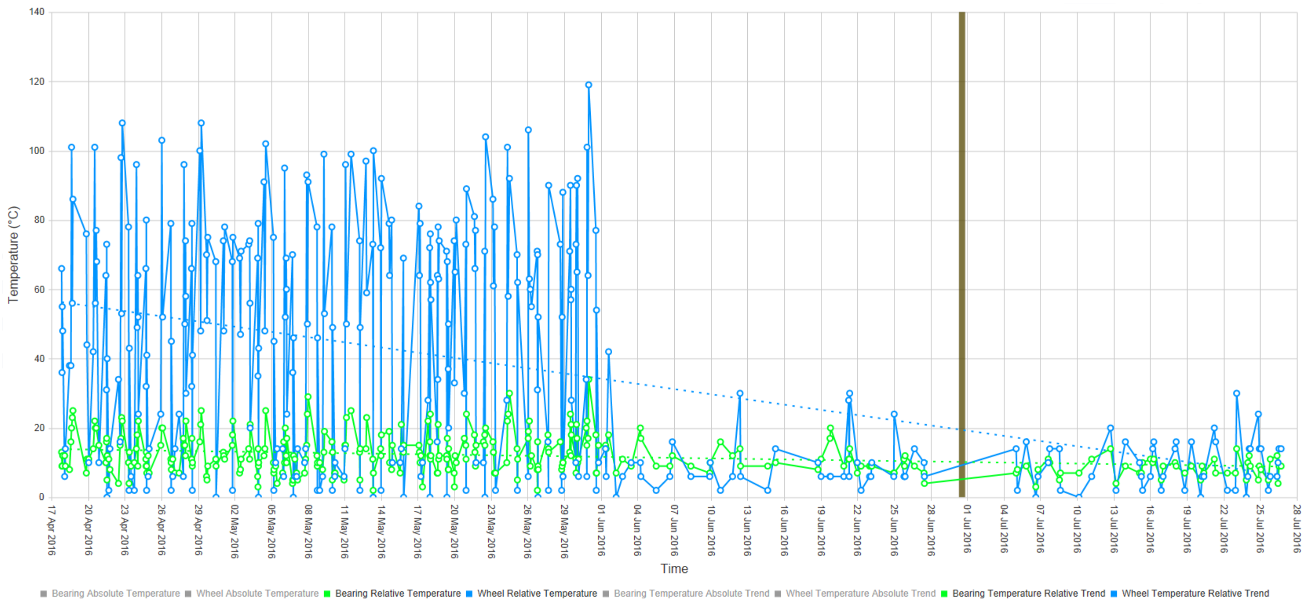


*1.1.1.1.7 B20270 Hot Box temperature trend – R1*

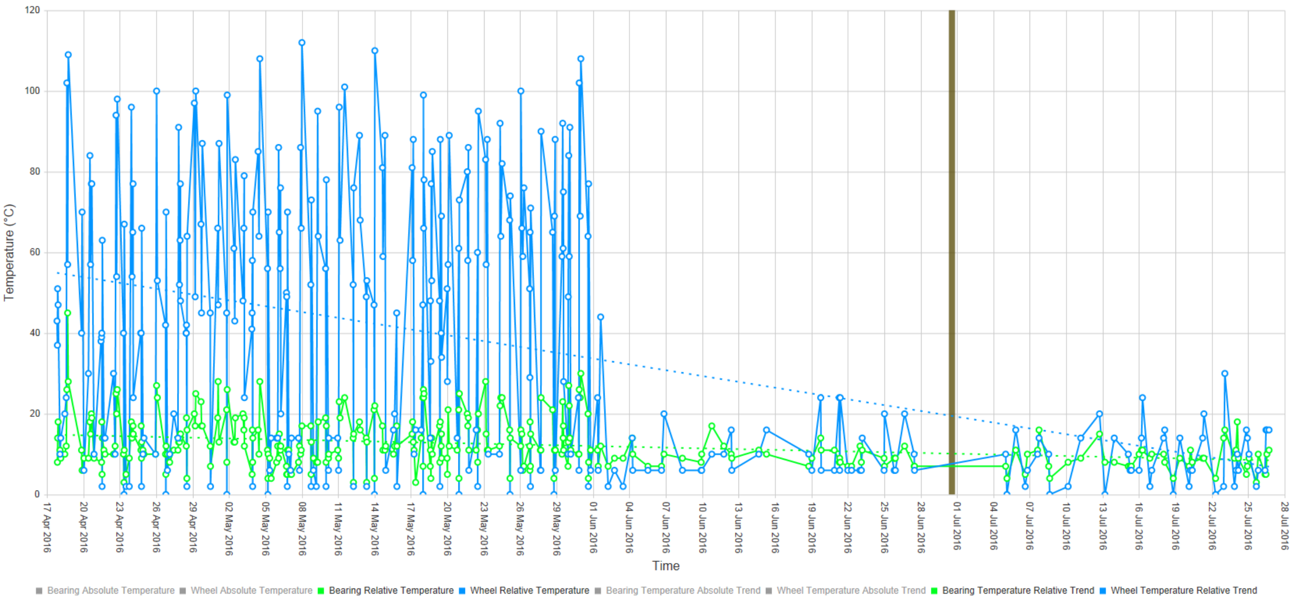


*1.1.1.1.8 B20270 Hot Box temperature trend – L1*

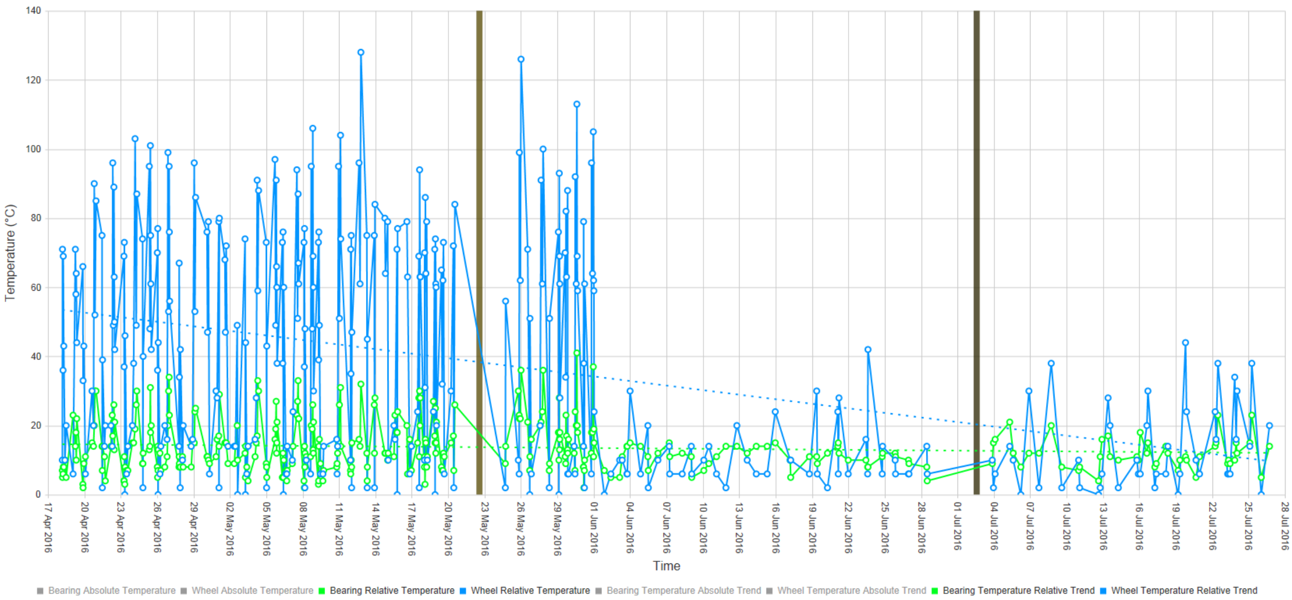


*1.1.1.1.9 B20045 Hot Box temperature trend – R1*

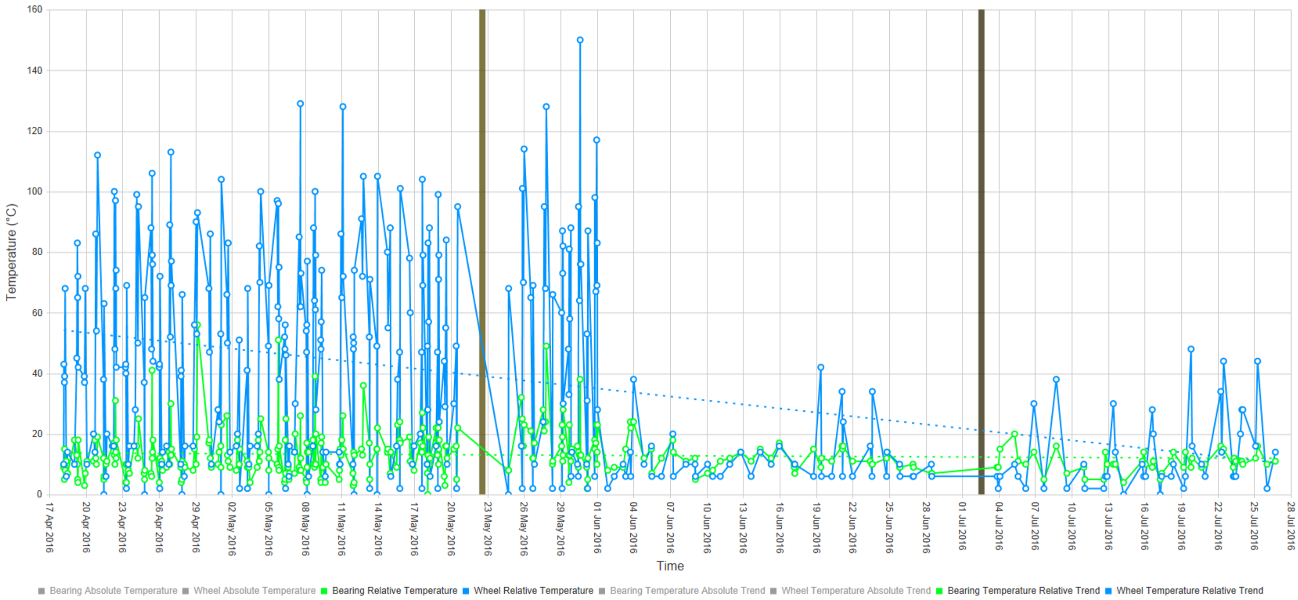


*1.1.1.1.10 B20045 Hot Box temperature trend – L1*

## A.4 RailBAM System

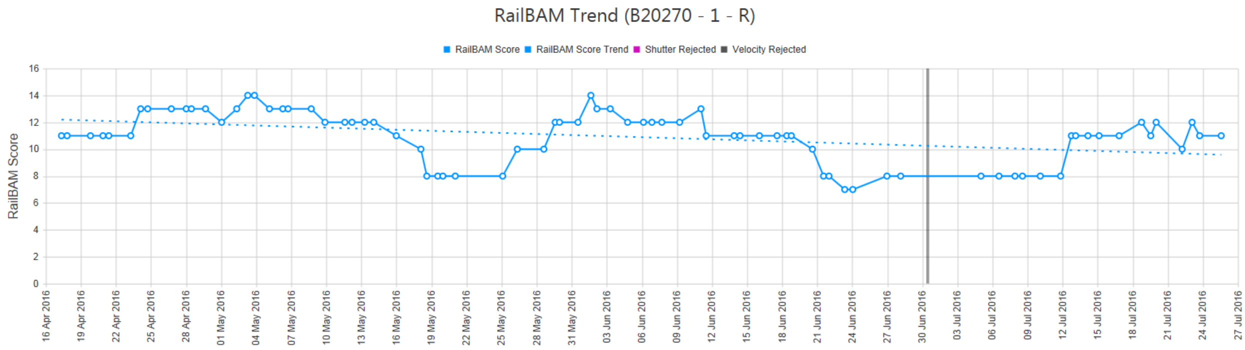


*1.1.1.1.11 B20270 RailBAM Trend R1*

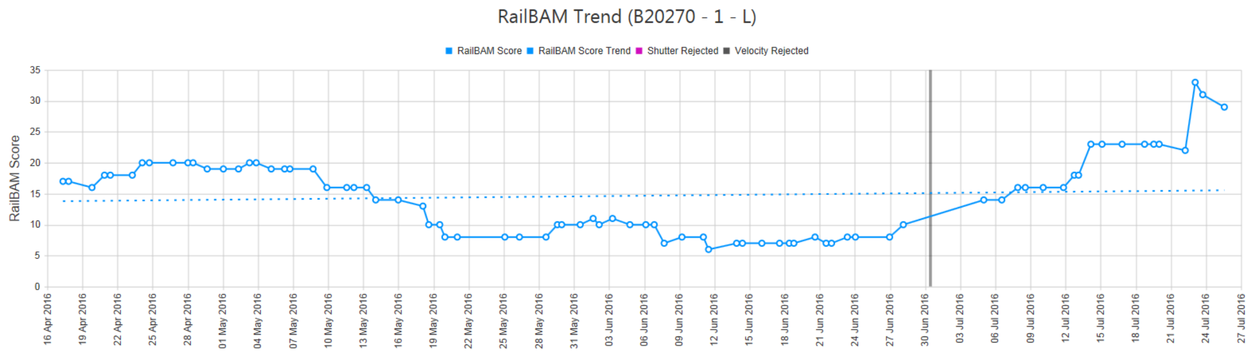


*1.1.1.1.12 B20270 RailBAM Trend L1*

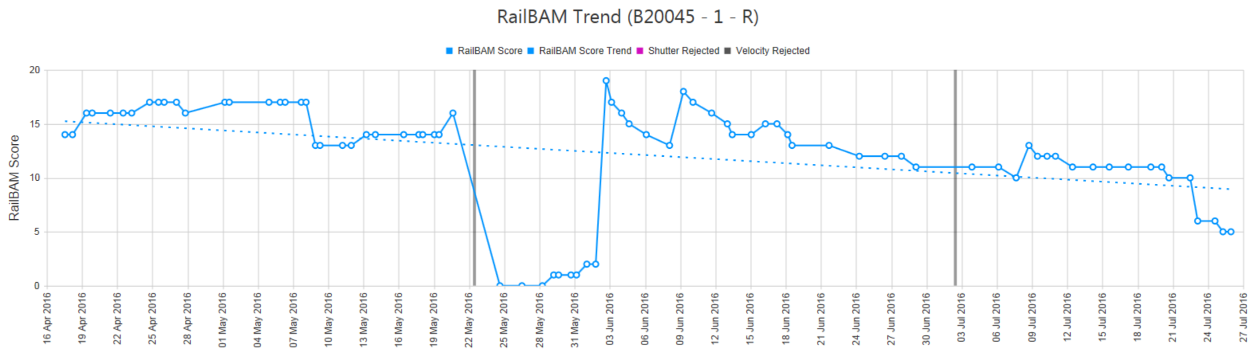


*1.1.1.1.13 B20045 RailBAM Trend R1*

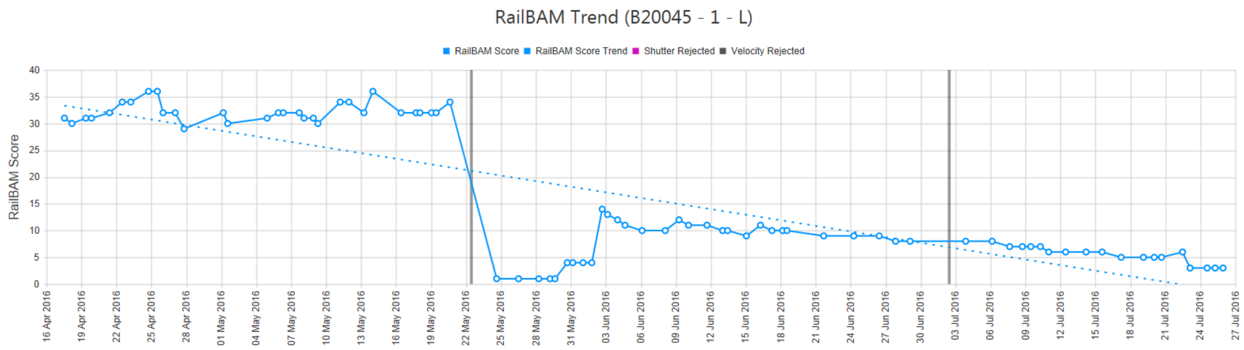


*1.1.1.1.14 B20045 RailBAM Trend L1*

## A.5 OCCM System

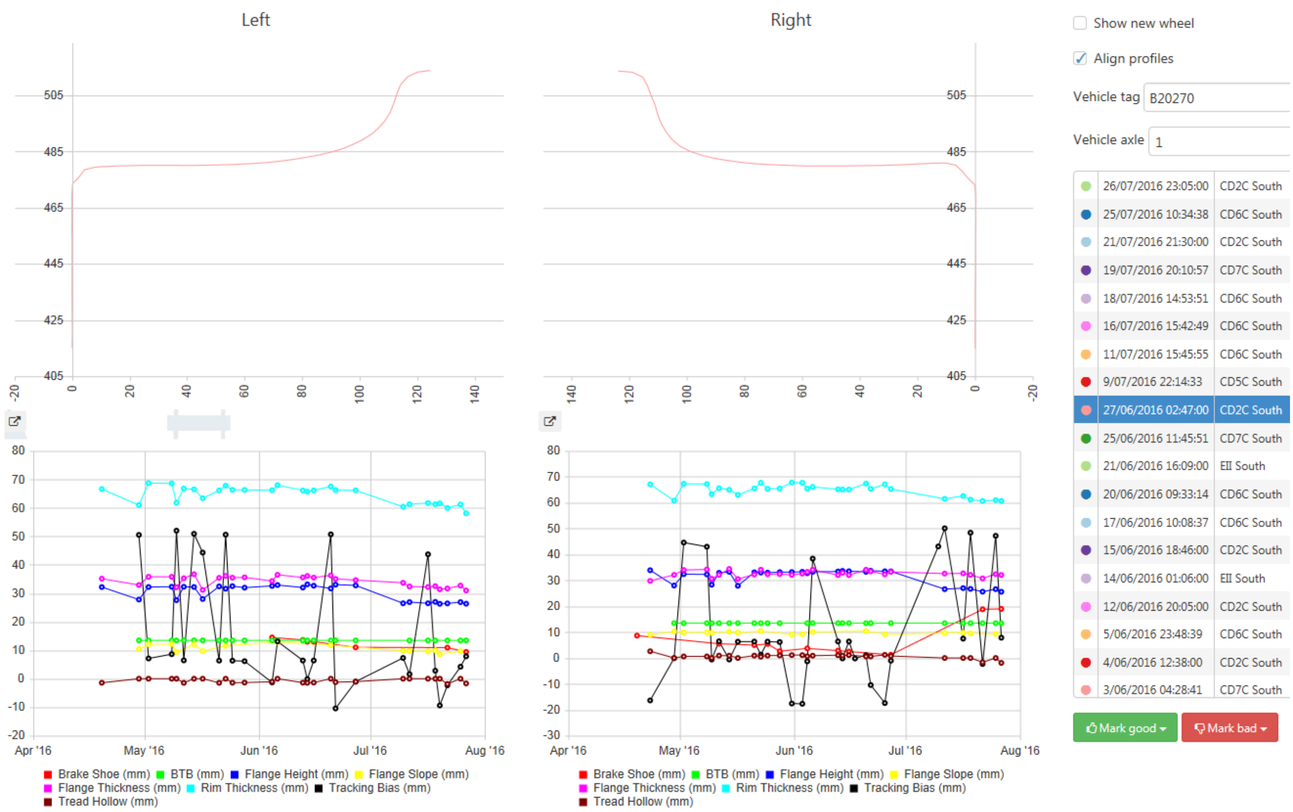

*1.1.1.1.15 B20270 Axle 1 OCCM reading*

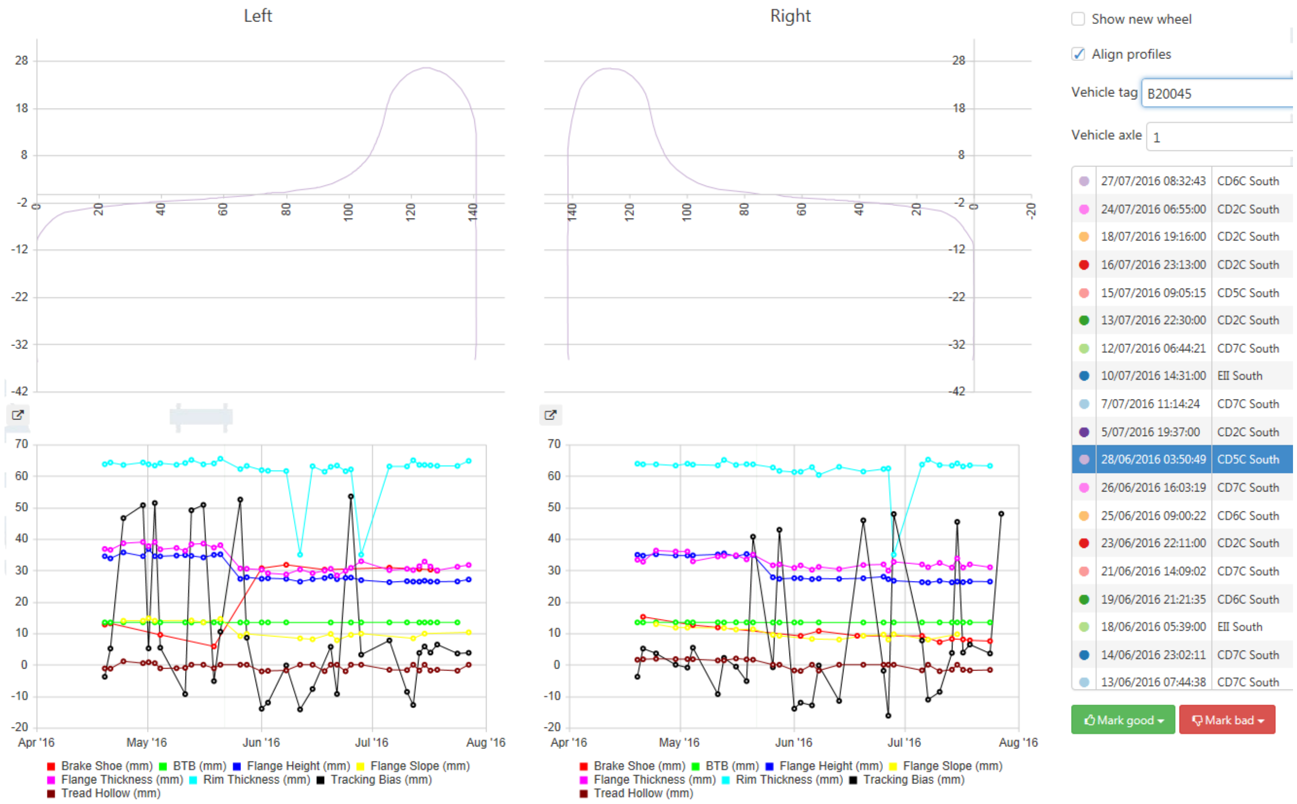


*1.1.1.1.16 B20045 Axle 1 OCCM reading*

## A.6 Track Map

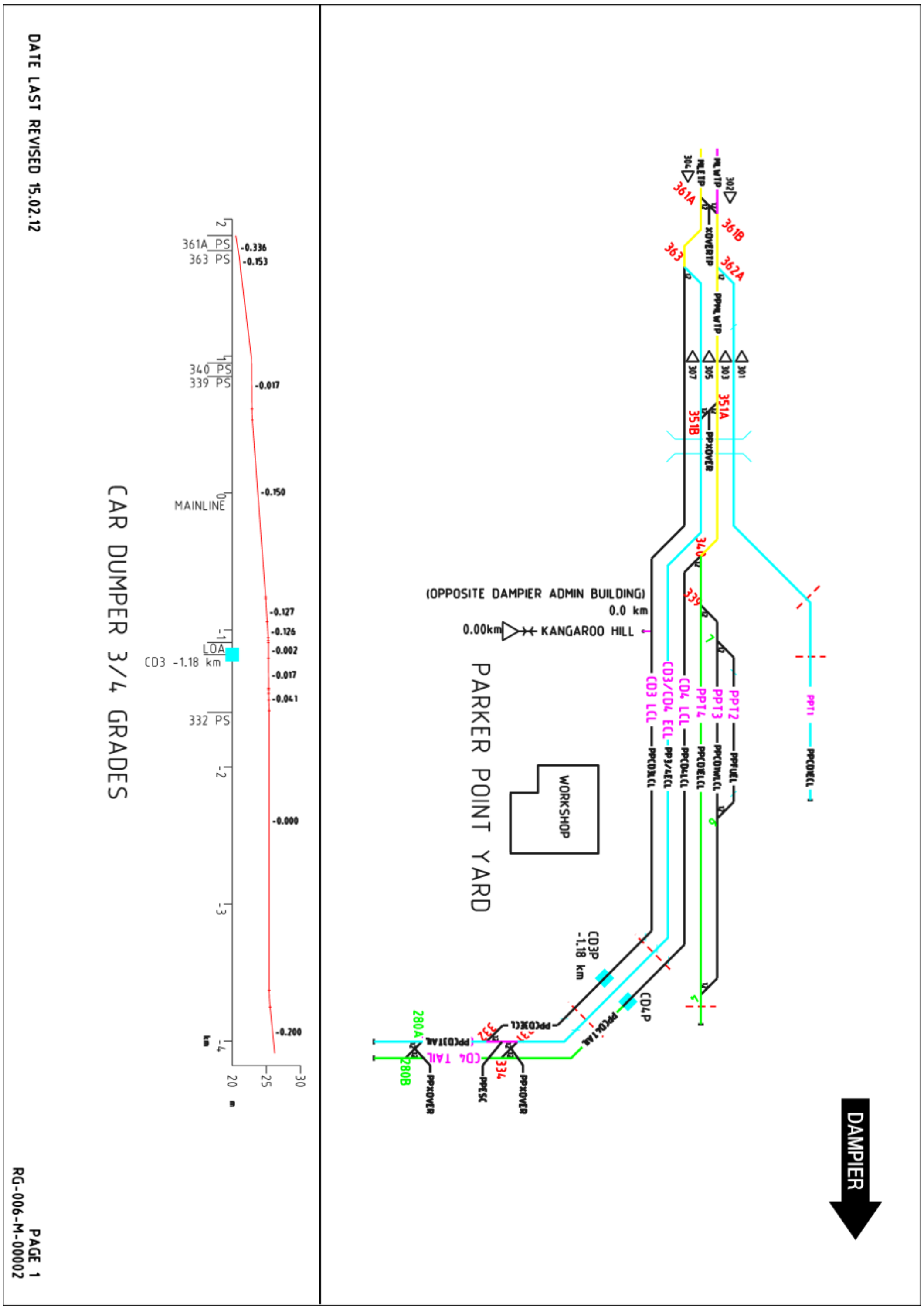

*1.1.1.1.17 Parker Point Yard track schematic*

## A.7 Track Maintenance History

The following track maintenance data has been gathered from the following SAP function locations:

- Parker Point Yard (3076PPYDML)

- Parker Point Yard Track (3076PPYDMLTRAC)
- Road 5 Sw340 to End CD4 LCL & Tail (3076PPYDMLROAD .RD05)

| Notification | Completion Date | Description |
|---|---|---|
| 25796033 | 02/08/2016 | CD4P LCL -0.050km Replace IRJ E/W Rails |
| 29550412 | 19/07/2016 | CD4P ECL Re-rail W/R week 27 Priority |
| 26570823 | 19/07/2016 | CD4P 16W Loaded Car Line Clean Track |
| 29263656 | 21/06/2016 | PPYARD CD4 fouled ballast Remove |
| 28663719 | 01/06/2016 | ^PPCD4LCL-1.523 W DW UT Defect |
| 28888315 | 30/05/2016 | CD4 outgo remove fouled ballast |
| 28011534 | 13/05/2016 | CD4 outgo remove fouled ballast |
| 28640982 | 23/04/2016 | Callout CD4 Inspect after derailment |
| 25908379 | 27/03/2016 | CD4P Derailment Remediation works |
| 22943243 | 14/12/2015 | # Repair track geometry issues CD4P |
| 26238354 | 23/10/2015 | PPCD4LCL -0.525 U/T DEFECT VSW IMMEDIATE |
| 23630402 | 04/05/2015 | ^S&L outgo end of CD4P |
| 21069979 | 09/12/2014 | ^Re-rail CD4PLCL -0.5 to -1.1 WR |
| 21103501 | 04/06/2014 | Vac Truck Tail Track CD4P every shut |
| 21622800 | 20/05/2014 | Trim Dumper Rails Ingo end CD4P |
| 18982780 | 13/04/2014 | Replace WR 1.39-1.72 km CD4LCL PP |
| 21153895 | 31/03/2014 | Remove DED from Ingo end CD4P |
| 21069969 | 24/03/2014 | Replace IRJ W/Rail CD4P Outgo end |
| 20181262 | 13/11/2013 | S&L CD4P Rerailer |
| 20575926 | 23/10/2013 | Profile Grind 361A & 361B |
| 18982755 | 20/09/2013 | Replace ER 1.39-1.72 km CD4LCL PP |
| 19340587 | 03/09/2013 | Install re-railers for engineering |
| 18919423 | 24/04/2013 | Ultrasonic Defect PPMLWTP W 1.260 DWH |
| 17011529 | 24/04/2013 | Rail Profile Monitoring Program MLE/ WTP |
| 18937013 | 14/04/2013 | Replace WR 2.3 to 3.65 km PPYD |
| 16935448 | 20/02/2012 | Weekly Switch Inspections PP YARD |
| 16802451 | 16/02/2012 | CD4P Dumper Rail Inspection |
| 16832141 | 13/02/2012 | DPR Weld out rail joints 362 switch |